The FEBS Journal

FEBS PRESS science publishing by scientists

Selectivity of the CUBAN domain in the recognition of ubiquitin and NEDD8

Luisa Castagnoli[1], Walter Mandaliti[2], Ridvan Nepravishta[2,3], Eleonora Valentini[4], Anna Mattioni[1], Radha Procopio[1,5], Marta Iannuccelli[1], Simona Polo[4,6], Maurizio Paci[2], Gianni Cesareni[1] and Elena Santonico[1]

1 Department of Biology, Tor Vergata University, Rome, Italy
2 Department of Chemical Sciences and Technologies, Tor Vergata University, Rome, Italy
3 School of Pharmacy East Anglia, University of Norwich, UK
4 IFOM, Fondazione Istituto FIRC di Oncologia Molecolare, Milan, Italy
5 Institute of Molecular Bioimaging and Physiology, CNR, Catanzaro, Italy
6 DIPO, Dipartimento di Oncologia ed Emato-oncologia, University of Milan, Italy

Keywords
cullin-RING ubiquitin ligases; NEDD8-binding domain; neddylation; nuclear magnetic resonance

Correspondence
G. Cesareni, Department of Molecular Genetics, Department of Molecular Genetics, University of Tor Vergata, Via della ricerca scientifica, 00133 Rome, Italy
Tel: +39 06 72594315
E-mail: Cesareni@uniroma2.it
and
E. Santonico, University of Tor Vergata, Via della ricerca scientifica, 00133 Rome, Italy
Tel: +39 06 72594307
E-mail: Elena.Santonico@uniroma2.it

Walter Mandaliti and Ridvan Nepravishta contributed equally to this work

(Received 23 July 2018, revised 25 September 2018, accepted 28 December 2018)

doi:10.1111/febs.14752

Among the members of the ubiquitin-like (Ubl) protein family, neural precursor cell expressed developmentally down-regulated protein 8 (NEDD8) is the closest in sequence to ubiquitin (57% identity). The two modification mechanisms and their functions, however, are highly distinct and the two Ubls are not interchangeable. A complex network of interactions between modifying enzymes and adaptors, most of which are specific while others are promiscuous, ensures selectivity. Many domains that bind the ubiquitin hydrophobic patch also bind NEDD8 while no domain that specifically binds NEDD8 has yet been described. Here, we report an unbiased selection of domains that bind ubiquitin and/or NEDD8 and we characterize their specificity/promiscuity. Many ubiquitin-binding domains bind ubiquitin preferentially and, to a lesser extent, NEDD8. In a few cases, the affinity of these domains for NEDD8 can be increased by substituting the alanine at position 72 with arginine, as in ubiquitin. We have also identified a unique domain, mapping to the carboxyl end of the protein KHNYN, which has a stark preference for NEDD8. Given its ability to bind neddylated cullins, we have named this domain CUBAN (Cullin-Binding domain Associating with NEDD8). We present here the solution structure of the CUBAN domain both in the isolated form and in complex with NEDD8. The results contribute to the understanding of the discrimination mechanism between ubiquitin and the Ubl. They also provide new insights on the biological role of a ill-defined protein, whose function is hitherto only predicted.

Introduction

Cells use the covalent attachment of small polypeptides to target proteins as a strategy to control protein function. Ubiquitination, the conjugation of Ubiquitin (Ub) to proteins, is the best characterized among these post-translation modifications and involves the formation of an isopeptide bond between the C-terminal glycine of

Abbreviations
CD, circular dichroism; CSP, chemical shift perturbation; CUBAN, cullin-binding domain associating with NEDD8; ITC, isothermal titration calorimetry; NEDD8, neural precursor cell expressed developmentally down-regulated protein 8; UBD, Ub-binding domain; Ubl, ubiquitin like; UIM, ubiquitin interaction motif.

ubiquitin and the lysine side chain in the target protein. The conjugation of ubiquitin is a three-step process that requires an ubiquitin-activating (E1) enzyme, an ubiquitin-conjugating (E2) enzyme and an ubiquitin ligase (E3). The modification mediates a plethora of biological processes such as DNA repair, transcription, signal transduction and intracellular membrane traffic [1]. Ubiquitin-like proteins (Ubls) are related to ubiquitin primarily by the ubiquitin superfold, called β-grasp fold [2] and by the basic set of enzymatic reactions, catalysed by E1, E2 and E3 enzymes, involved in the conjugation process. The functional consequences of these modifications are distinct, depending on the Ubl that is added and on the characteristics of the substrate.

Among all the Ubl proteins, NEDD8 shares the highest homology with ubiquitin (~ 57% identity and ~ 76% similarity). In spite of this, the NEDD8 pathway is clearly insulated since its substrates are primarily members of the cullin (CUL) family [3], while on the other hand, ubiquitin is conjugated to virtually every protein. The neddylation of cullins requires a NEDD8-specific heterodimeric E1 enzyme, composed of APPBP1 and UBA3 proteins, the E2 enzyme UBC12 and the E3 enzyme RING-box protein 1/2 (Rbx1/2). Many studies have clearly demonstrated that small but substantial differences in ubiquitin and NEDD8 sequences guarantee the clear discrimination between substrates directed towards ubiquitination or neddylation [4–6]. This specificity is primarily based on the different amino acid occupying position 72, indeed, the presence of an arginine (Arg72) in ubiquitin, instead of the evolutionary conserved alanine in NEDD8 (Ala72) prevents misactivation of ubiquitin due to the repulsion from UBA3's Arg190 localized in the binding pocket [7–10] Similarly, ubiquitin chains carrying the R72A mutation are a better substrate for the deneddylating enzyme NEDP1, while they are less efficiently cleaved by the ubiquitin-specific protease HAUSP [9–11]. The outcome of these selective mechanisms is that the conjugation of ubiquitin is strictly limited to its enzymatic sets. On the contrary, the Ubl NEDD8 shows to be qualitatively competent in the interaction with the enzymes specific for ubiquitin. Nevertheless, due to significantly slower kinetics, these reactions are rather inefficient, suggesting that promiscuity of NEDD8, differently from ubiquitin, is not forbidden but strongly disfavoured [10,12].

Cells use protein tagging by ubiquitin and ubiquitin-like peptides as a sort of code deciphered by receptors that interpret these signals and transduce them to the appropriate intracellular responses. In accordance with the high similarity, NEDD8 retains many determinants that enable ubiquitin the ability to target proteins to degradation. In particular, the hydrophobic patch (comprising residues Leu8-Ile44-His68-Val70), which is responsible for most of the interactions with structurally diverse Ub-binding domains (UBDs), is perfectly conserved in NEDD8. As a consequence, different UBDs show hardly any preference for binding ubiquitin or NEDD8. Indeed, available evidence supports a network of complex and hitherto poorly understood promiscuous interactions between Ubl and ubiquitin-binding domains. Starting from the evidence that NEDD8 interacts with proteasome ubiquitin-shuttle and receptor proteins comparably to ubiquitin [13], several examples attest a promiscuous role of NEDD8 in degradative, regulatory and protein-sorting/trafficking functions, which are processes typically regulated by the ubiquitin pathway. For example, NEDD8 binds the ubiquitin interaction motifs (UIM) in Eps15, Hrs and STAM [14]. The UBA-UBX protein UBXD7, in addition to binding ubiquitin conjugates, interacts with neddylated CUL2 through a direct interaction between its UIM motif and conjugated NEDD8 [15,16]. Analogously, the UBA domain of TRIAD1 is responsible for the association with neddylated cullin-RING ubiquitin ligases [17] and the MIU (motif interacting with ubiquitin) domain of RNF168 recognizes ubiquitination signals as well as poly-neddylated Histone 4 [18]. Two independent screenings revealed the presence of leucine-rich sequences acting as unique NEDD8-binding motifs in NUB1 and in its splicing variant NUB1L. These motifs are embedded in the UBA domain within both variants and act by recruiting NEDD8 and its conjugates to the proteasome for degradation [19]. Moreover, the NUB1 and NUB1L UBA domains have been shown to bind to the small Ubl molecule FAT10 as well, most likely for their high sequence and structural similarities, resulting in the increased degradation of FAT10 and FAT10-modified cargos [20]. Lately, multiple NEDD8-binding sites have been identified in the HECT domain of the Smurf E3 ligases [21]. Intriguingly, both Smurf1 and Smurf2 also contain ubiquitin-binding sites but, differently from the aforementioned examples, they are distinct from the NEDD8-binding sites. Even more interestingly, the authors demonstrated that, in addition to mediate noncovalent interactions with NEDD8, the Smurf1 HECT domain catalyses its own neddylation, having the effect of increasing its ubiquitination activity [22]. It appears, therefore, that there is still some confusion if not an apparent contradiction between, on the one hand, the existence of highly specific mechanisms that allow the cell to discriminate between ubiquitin and the highly related NEDD8 and, on the other hand, the evidence that several biological mechanisms involving ubiquitin accept a certain degree of redundancy when dealing with NEDD8.

In the present work, we have investigated the binding preferences of NEDD8 and ubiquitin by panning a human brain phage displayed cDNA library. The characterization of several Ubl-binding domains identified a NEDD8-binding domain in the KHNYN protein. This new domain, that we have named CUBAN (Cullin-Binding domain Associating with NEDD8), binds to neddylated cullins and shows a clear preference for NEDD8 over monomeric ubiquitin. Structural analysis by NMR spectroscopy revealed a novel three alpha-helix bundle domain. Our data indicate that both hydrophobic and polar residues contribute to the interaction surface between CUBAN and NEDD8.

Results

Identification of ubiquitin and NEDD8-binding domains by phage lambda display

To identify peptides or domains that bind either ubiquitin or NEDD8, we panned a human brain cDNA library whose translation products are displayed on the capsid of bacteriophage lambda [23]. After two or three panning cycles, the sequences of the cDNA inserts of 100 randomly selected clones were determined and the amino acid sequence of the translation products inferred (Fig. 1). Table 1 reports the list of nonredundant protein fragments selected using ubiquitin or NEDD8 as baits. The DNA sequence of 65 clones selected in the ubiquitin panning experiments identified a total of 14 cDNA coding sequences. Most of the selected cDNA fragments encode peptides whose sequence matches the consensus of already characterized UBD families. These include two UIM motifs (PSMD4, OTUD5), six UBA domains (RAD23, SQSTM1, UBQLN1, USP13, UBL7, CBLB), one UBZ domain (TAX1BP1), the ZnF domains of ZNF313 and YAF2 and the UBM domain of POLI. In addition, we selected the C-terminal ends of two evolutionary related proteins named N4BP1 (NEDD4-binding protein 1) and KHNYN (KH and NYN domain-containing protein). Although N4BP1 have been shown to be ubiquitinated in cells and to associate with ubiquitin, the characterization of its UBD, in terms of domain family and mapping, is missing [24,25]. Finally, no information is currently available regarding the ubiquitin-binding properties of KHNYN. The panning with the NEDD8 bait yielded 54 independent clones displaying overlapping protein fragments of five putative binding partners, all of them being also selected in the previous panning experiment: RAD23A, CBL-b, POLI, UBQLN1 and KHNYN. Interestingly, two of the five binding partners, the UBA domains of Rad23A and UBQLN1, have already

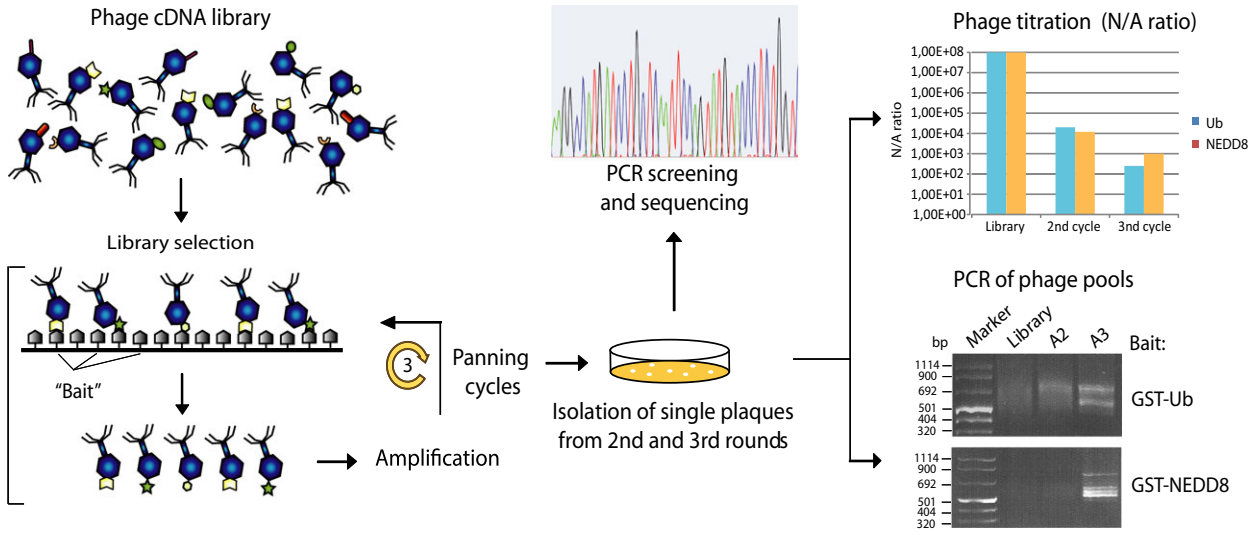

Fig. 1. Schematic representation of the phage display approach. A cDNA library containing 108 independent cDNA clones expressed by fusion to the carboxyl end of the D capsid protein were used to identify binding partners of ubiquitin and NEDD8. After each selection cycle the ratio between input and recovered phage titres (N/A) were determined. The N/A ratio for the selection with Ubiquitin (blue bars) and NEDD8 (orange bars) is shown in the graph. To monitor the phage enrichment, the phage pools from the second and third round as well as the phage library were analysed by PCR using oligonucleotides for the amplification of the polylinker region. Phages attached to the bait resin after the second and third round of selection were plated on agar plates and clones randomly selected for characterization of the cDNA inserts by sequencing.

Table 1. Ubiquitin and NEDD8 binding domains identified by phage lambda display. Clones selected by both phage display experiments were classified as only selected by Ubiquitin (Ubiquitin) or interactors commons to both baits (Ubiquitin/NEDD8). For each prey the human protein name, the uniprot code and the selected amino acid region are shown.

Ubiquitin/NEDD8	Uniprot	Amino acid region	Ubiquitin	Uniprot	Amino acid region
RAD23A	P54725	298–363	USP13	Q92995	689–769
POLI	Q9UNA4	643–715	SQSTM1	Q13501	385–440
UBQLN1	Q9UMX0	516–589	UBL7	Q96S82	283–380
KHNYN	O15037	598–678	N4BP1	O75113	813–896
CBLB	Q13191	916–982	TAX1BP1	Q86VP1	741–789
			ZNF313	Q9Y508	192–228
			YAF2	Q8IY57	19–54
			OTUD5	Q96G74	392–427
			CBLB	Q13191	916–982
			PSMD4	P55036	271–377

been described as NEDD8 interactors [13]. Concluding, the phage display panning approach did not provide evidence for a protein domain strictly specific for NEDD8, thus confirming that evolutionary conserved features in ubiquitin and NEDD8 mediate the recognition by the majority of UBDs.

The identity of the residue at position 72 is critical in determining the preference of UBDs for ubiquitin or NEDD8

The results of the phage display approach suggested that some ubiquitin-binding domains hardly bind NEDD8. Since this was reminiscent of the inefficient utilization of NEDD8 by the ubiquitin-conjugating enzymes, which is mainly determined by the residue at position 72 (Fig. 2A), we asked whether position 72 in NEDD8 could also underlie the Ubl/ubiquitin recognition specificity by different UBDs. To this end, we expressed the selected domains as GFP fusions by transient transfection of the 293Ph cell line and we investigated by pull-down assays their binding to the GST-tagged wild-type and mutant versions of ubiquitin and NEDD8: UBQwt, UBQ I44A, NEDD8wt, NEDD8 I44A and NEDD8 A72R (Fig. 2B). As shown, we could arrange the set of UBDs in three different groups: in the first one, including OTUD5, ZNF313, SB132 and SQSTM1, the GFP-tagged constructs efficiently bound ubiquitin and the interaction was severely affected by mutating the Ile44 key residue in the hydrophobic patch. No association with NEDD8 could be observed. Members of this group can be defined as 'not-promiscuous'. The domains of the second group, including those of N4BP1, RAD23A, IOTA, YAF2 and UBL7 showed a variable binding efficiency for NEDD8. Interestingly, the NEDD8 binding affinity was strengthened by the A72R mutation that makes the NEDD8 carboxyl-terminal tail more similar to ubiquitin. These findings suggest that, among the residues that are divergent in the NEDD8 and ubiquitin amino acid sequences, Ala72 is responsible for the weak binding of NEDD8 to the UBDs that can potentially recognize both post-translational modifications. The I44A mutation abrogated the interaction with UBDs in both ubiquitin and NEDD8, thus confirming the essential role of the conserved hydrophobic patch. This group can be considered potentially 'promiscuous'. A single member, KHNYN, which shows a clear preference for NEDD8 over ubiquitin, forms the third group. Interestingly, the A72R mutation partially affects binding to NEDD8, suggesting that the acquisition of ubiquitin features interferes with the ability of this domain to bind its specific target in KHNYN. This group, having KHNYN as its single member, can be defined as 'selective'. Collectively, these results portray a continuum landscape of recognition specificities that determines the preference for ubiquitin and NEDD8 by ubiquitin-binding domains and indicate the role of the residue at position 72 in modulating this specificity.

We next analysed the interaction of the selected binding domains in a eukaryotic cell system. To perform this analysis, the cDNA fragments identified by phage display were expressed as GST fusions and assayed in pull-down experiments for the ability to associate with ubiquitinated and neddylated substrates. To facilitate the identification of NEDD8 substrates, we used a T-Rex-flag-NEDD8 cell line expressing flag-tagged NEDD8 under the control of a tetracycline-inducible promoter. The cell extract analysed by western blotting with anti-flag antibody (Fig. 3A) shows a ladder of neddylated substrates, with the major bands corresponding to proteins with molecular weights in the range of 90–130 kDa. The expression of tagged

A

```
hNEDD8   MLIKVKTLTGKEIEIDIEPTDKVERIKERVEEKEGIPPQQQRLIYSGKQMNDEKTAADYK
hUBC     MQIFVKTLTGKTITLEVEPSDTIENVKAKIQDKEGIPPDQQRLIFAGKQLEDGRTLSDYN
         * * ******* * :::**:*.:*.:* ::::******:*****::***::* :* :**:

hNEDD8   ILGGSVLHLVLALRGGGGLRQ      81
hUBC     IQKESTLHLVLRLRGG-----      76
         *   *.***** ****
```

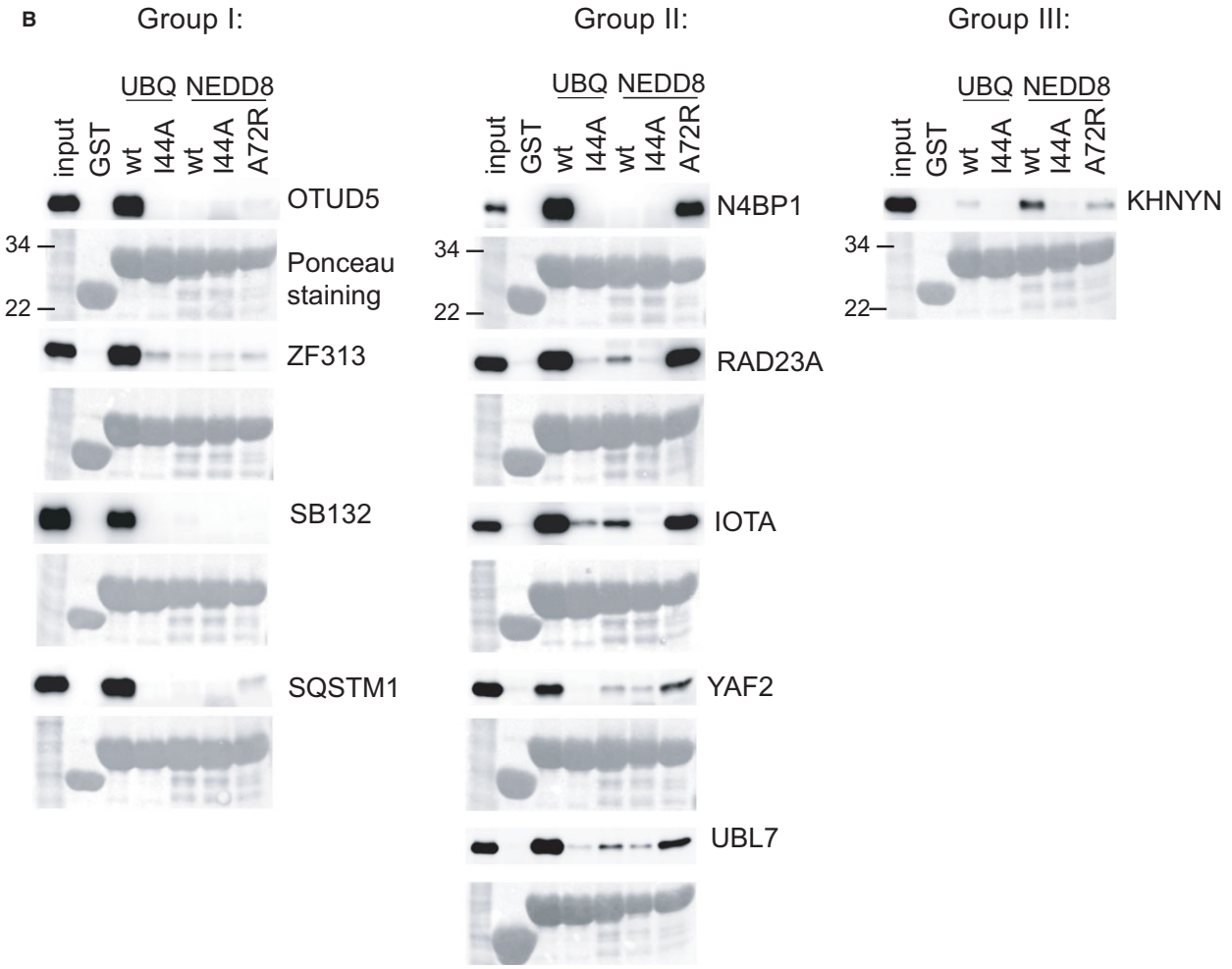

Fig. 2. (A) Sequence alignment between human NEDD8 and ubiquitin performed with CLUSTAL OMEGA (Science Foundation Ireland, Dublin, Ireland); a match of the amino acid residue is indicated by '*' (identical), ':' (similar) or '.' (weakly similar properties). Residues that constitute the hydrophobic patch are shown in bold (L8, I44, H68 and V70). Position 72 is shown in bold red. (B) Differences in the binding preferences of selected clones revealed by the Ala72Arg NEDD8 mutant. The cDNA fragments selected by phage display were cloned as GFP fusions and transiently transfected in 293Ph cells. Cell extracts were used in pull-down experiments performed using as baits the indicated GST fusion proteins. Samples were analysed by SDS/PAGE and immunoblotting with anti-GFP antibody. Ubiquitin-binding domains were clustered in three groups as described in the text.

NEDD8 is significantly lower than the endogenous levels, thus excluding any atypical neddylation (Fig. 3B). T-Rex-flag-NEDD8 cell lysates were therefore incubated with the purified proteins bound to glutathione-Sepharose beads and affinity-purified proteins were analysed by western blotting with anti-flag antibody (Fig. 3C). As observed, the purified UBDs considerably differ in their ability to bind neddylated

substrates, KHNYN being the one displaying the highest binding efficiency. In addition, the UBD of KHNYN was the only one able to bind both neddylated substrates and unconjugated flag-NEDD8, as detected by longer exposure. Equal amounts of precipitated proteins were analysed by western blotting with anti-ubiquitin. Again, differences in binding to ubiquitinated substrates can be highlighted, which do not always match those observed with neddylated substrates. Finally, we assayed the binding of the GST-purified ubiquitin-binding domains against purified monomeric ubiquitin and NEDD8 (Fig. 3D), both revealed through incubation with the anti-ubiquitin antibody P4D1 that cross-react with NEDD8 (Fig. 4) [26]. The result confirms a clear preference of KHNYN for NEDD8. Concluding, all the domains selected by phage display share the ability to bind multi- and poly-ubiquitinated proteins; some also bind neddylated proteins. On the other hand, the ubiquitin-binding domain identified in KHNYN is unique in showing a preferential binding to both NEDD8 monomers and neddylated substrates.

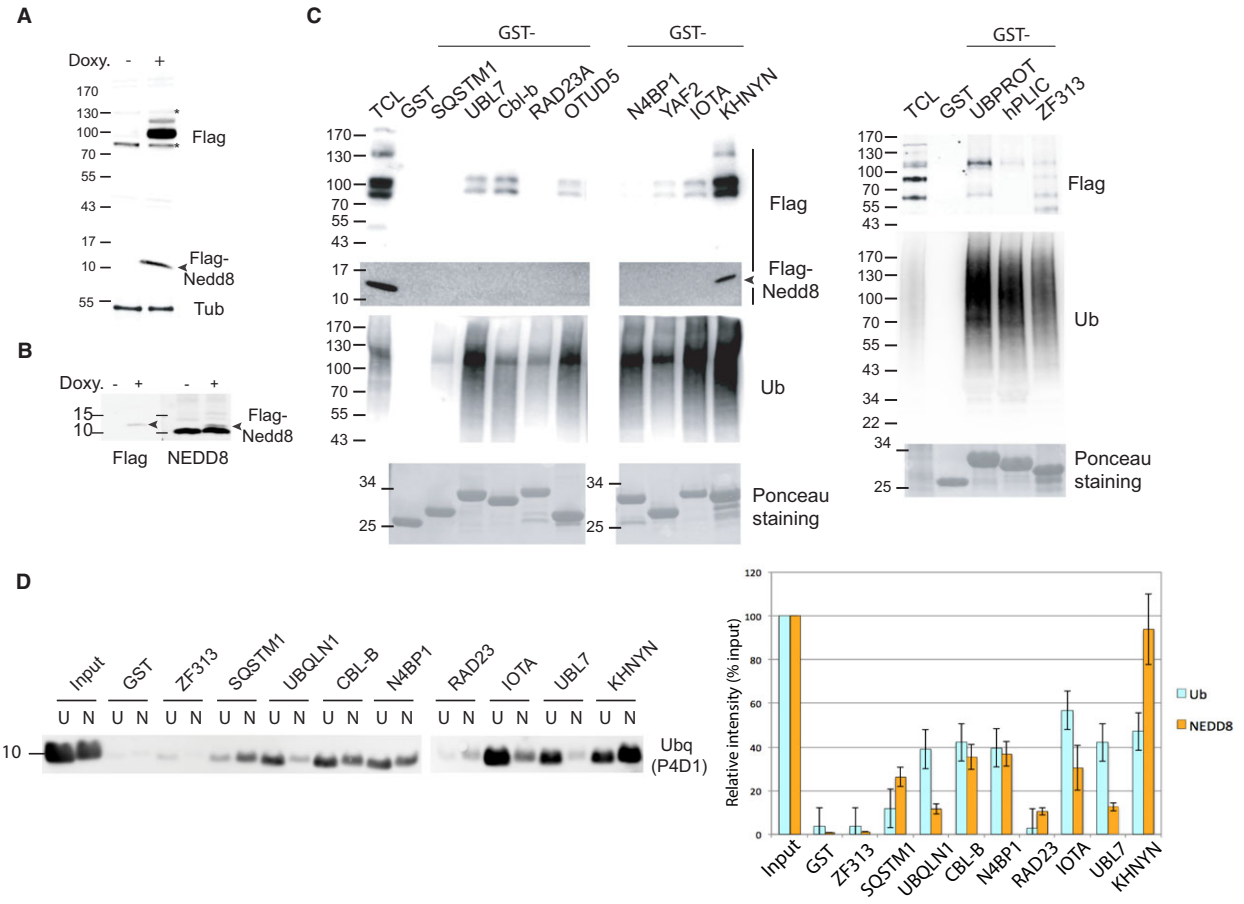

Fig. 3. (A) Incubation of the Flp-In 293 T-Rex cell line with doxycycline 100 nM for 18 h induces the appearance of the flag-tagged NEDD8 monomer and high-molecular weight proteins. Equal amounts of cell extracts were analysed by SDS/PAGE and western blotting with anti-flag antibody. Asterisks indicate unspecific signals of the anti-flag antibody. (B) Flag-tagged monomeric NEDD8 is expressed at very low levels compared to the endogenous protein. Equal amounts of T-Rex flag-NEDD8 incubated with doxycycline or untreated were analysed by SDS/PAGE and western blotting with anti-flag or anti-NEDD8 antibodies. Arrowheads indicate endogenous NEDD8 and the doxycycline-induced flag-NEDD8 protein. (C) Pull-down experiments from doxycycline-induced T-Rex flag-NEDD8 cells were performed with the GST recombinant proteins obtained by subcloning the selected Ubiquitin- and NEDD8-binding domains in the pGex2TK vector. Samples were assayed for the interaction with neddylated and ubiquitinated substrates. Precipitated proteins were analysed by SDS/PAGE and western blotting with anti-flag and anti-Ubiquitin antibodies. In the left panel, a longer exposure reveals the interaction with flag-NEDD8 monomers. (D) The indicated GST recombinant proteins were incubated with equal amounts of monomeric ubiquitin and NEDD8. Samples were analysed as previously and immunoblotted with the anti-ubiquitin antibody P4D1 which cross-reacts with NEDD8. Densitometry calculations of bands from $n = 2$ experiments were made using IMAGEJ software (Research Services Branch, National Institute of Mental Health, Bethesda, MD, USA) and signals were expressed as percentage of the input intensity. Data are shown as mean ± SD.

A novel binding domain in N4BP1 and KHNYN shows a different specificity versus ubiquitin and NEDD8

N4BP1 and KHNYN are evolutionarily related and share a similar domain organization [27]. Both the C-terminal ends of N4BP1 and KHNYN, encompassing respectively residues 813–896 and 598–678, were selected in our panning experiments, despite displaying different binding preferences. The ~ 80-residue long C-terminal ends share a region of homology (40% residue identity and 57% similarity) at the carboxyl terminus while the amino-terminal regions are unrelated (Fig. 5A). Interestingly, the secondary structure prediction performed with Jpred4 (http://www.compbio.dundee.ac.uk/www-jpred/) [28] reported a bundle of three α-helices occupying the last 50 aa of both C-terminal regions, a fold that is typical of many ubiquitin-binding domains. By performing a SMART search [29,30], no previously described domain could be identified in the region of KHNYN selected by phage display. On the other hand, a CUE (Coupling of Ubiquitin conjugation to ER degradation) domain was detected at the C-terminal end of the N4BP1 ubiquitin-binding fragment, but with significance score lower than the required threshold. To investigate the binding properties of the KHNYN C-terminal region, we engineered and expressed two smaller constructs spanning residues 609–678 and 627–678, respectively, (Fig. 5A, see schematic representation) and we tested them by pull-down assay against a cellular extract of T-Rex-flag-NEDD8 cells (Fig. 5B, upper panel) or by incubating the GST fusions with purified NEDD8 (Fig. 5B, lower panel). The results showed that the C-terminal 52 residues of KHNYN bind NEDD8 and neddylated substrates with an efficiency that is comparable to that of the region selected by phage display. Even though the pull-down approach gives a qualitative rather than a quantitative indication, this observation supports the conclusion that the minimal binding region for the interaction with NEDD8 and NEDD8 substrates is indeed the one here identified. Moreover, we preferred to reduce the minimal length of the sequence in study also in prospective of a structural approach (see below) that appeared difficult to perform by using amino acidic ranges longer than the region stably helically folded.

To further confirm that the molecular determinants governing NEDD8 recognition are found in the C-terminal 52 residues of KHNYN, we generated two chimeras by swapping the amino acid regions corresponding to the three α-helices. The first chimeric construct, KN, contains the N-terminal unique region of KHNYN (aa 598–634) and the α-helices of N4BP1 (aa 854–896), while in the NK construct the last three helices of KHNYN (aa 635–678) are fused to the N-terminal region of N4BP1 (aa 813–852) (Fig. 5C). The purified recombinant proteins were analysed by pull-down assays for the ability to bind neddylated substrates in the T-Rex-flag-NEDD8 cells. As shown, the chimeric construct NK retains the properties of wild-type KHNYN, as it is able to bind to conjugated and monomeric NEDD8. Conversely, the GST-KN recombinant chimera showed the same binding specificity as N4BP1. These findings imply that the KHNYN α-helical carboxyl-terminal domain contains the determinants for binding to neddylated substrates. Finally, to map more

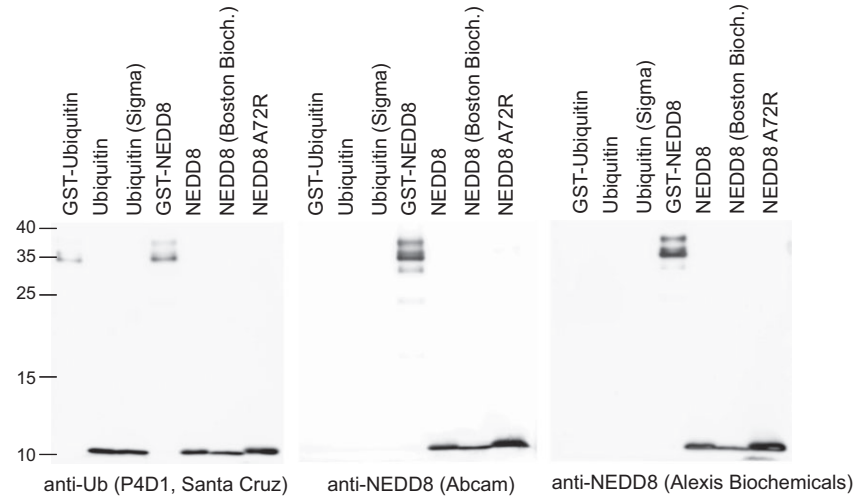

Fig. 4. Equal amounts of GST-Ubiquitin, Ubiquitin (homemade and commercially distributed from Sigma), GST-NEDD8, NEDD8 wild-type (homemade and commercially distributed from Boston Bioch.) and NEDD8 A72R were analysed in triplicate by SDS/PAGE and immunoblotting with anti-Ubiquitin (P4D1; Santa Cruz), anti-NEDD8 (Abcam) and anti-NEDD8 (Alexis Biochemicals, San Diego, CA, USA).

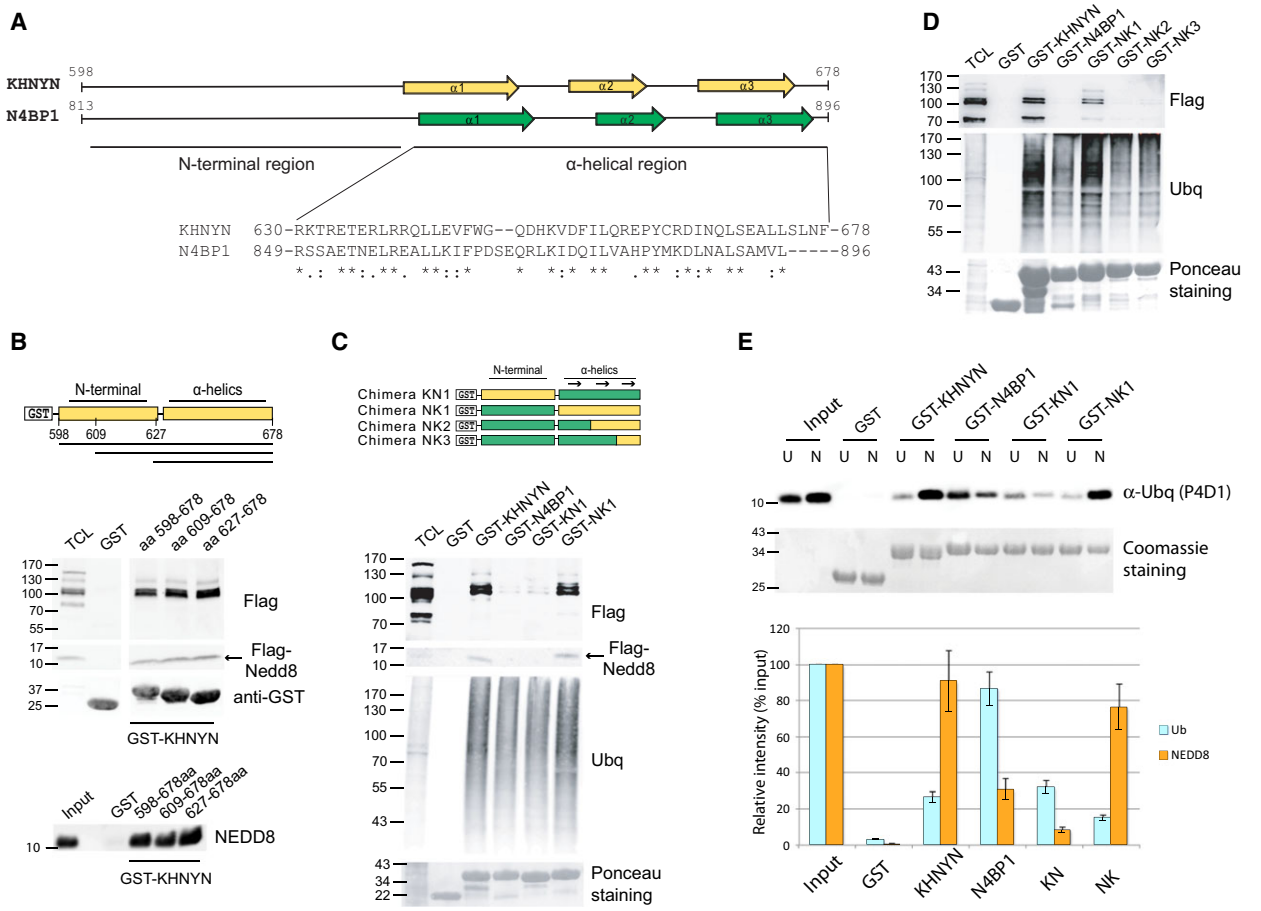

Fig. 5. The C-terminal ends of KHNYN and N4BP1 present a novel evolutionary related binding domain showing different binding properties towards Ubiquitin and NEDD8. (A) Secondary structure prediction performed with JPred4 server using the amino acid regions of KHNYN and N4BP1 revealed the presence of three α-helices preceded by an unstructured region. Identity and similarity values among the C-terminal residues of KHNYN and N4BP1 were performed with CLUSTAL OMEGA [57, 58]; a match of the amino acid residue is indicated by '*' (identical), ':' (strongly similar properties) or "." (weakly similar properties). (B) The region spanning residues 627–678 mediates the interaction with conjugated and free NEDD8 expressed in T-Rex flag-NEDD8 cells (upper panel) and with the purified molecule (lower panel). (C) Swapping of the entire helical regions was performed to generate the chimeric constructs KN and NK. The recombinant constructs expressed as GST fusions were assayed in pull-down experiments to evaluate the interaction with neddylated and ubiquitinated substrates from T-Rex flag-NEDD8 cells. (D) Similar experiment as in (C) but using the chimeric constructs NK1, NK2 and NK3, the last two obtained by swapping respectively at Gln649 in KHNYN (Gln870 in N4BP1) and at Tyr662 in KHNYN (Tyr883 in N4BP1). (E) The interaction with purified monomeric NEDD8 (N) and ubiquitin (U) was analysed by pull-down and immunoblotting with anti-Ubq from Santa Cruz (P4D1). Densitometry calculations of bands from $n = 2$ experiments were made using IMAGEJ software and signals were expressed as percentage of the input intensity. Data are shown as mean ± SD.

finely the determinants of the KHNYN domain binding specificities, we generated two additional chimeras where the N4BP1 second and third C-terminal α-helices were swapped with the KHNYN counterparts (Fig. 5D). Both constructs efficiently bound ubiquitinated substrates, as the wild-type N4BP1, but neither was able to bind NEDD8 substrates underlining the important role played by the first α-helix in the recognition of NEDD8. This conclusion is reinforced by an experiment where the chimeric constructs are tested for their ability to bind monomeric ubiquitin or NEDD8 (Fig. 5E). Thus, despite the high similarity in their C-terminal ubiquitin-binding regions, KHNYN and N4BP1 have diverged in their ability to discriminate ubiquitin from the most similar ubiquitin-like NEDD8.

The interaction of the KHNYN protein with cullins requires neddylation and is independent from ubiquitination

To definitely confirm that the CUBAN domain retains the same binding properties in the full-length protein,

we performed pull-down and co-immunoprecipitation experiments (Fig. 6A–C). HeLa cells transfected with flag-tagged KHNYN were lysed and the supernatants incubated with ubiquitin and NEDD8 fused to the GST or with the GST alone. As shown in Fig. 6A, analogously to the isolated CUBAN domain, the full-length protein shows a marked preference for NEDD8. The essential role of the CUBAN domain in the recognition of NEDD8 and neddylated substrates was also confirmed by coimmunoprecipitation in HeLa cells transiently transfected with flag-KHNYN (Fig. 6B). The immunoprecipitates were analysed by SDS/PAGE and immunoblotting with anti-NEDD8 antibody. The result showed that the interaction of KHNYN with neddylated cullins was abrogated following deletion of the CUBAN domain. We then investigated the interaction of the NEDD8-binding domain of KHNYN with CUL1 and CUL2 endogenously expressed in T-Rex-flag-NEDD8. The C-terminal end of KHNYN was tested in a pull-down assay together with two different ubiquitin-binding sequences (the UIM motif and the VHS domain of STAM2 protein) and the GST alone. As shown in Fig. 6C, several neddylated substrates were affinity purified by the GST fusion of the KHNYN ubiquitin-binding domain, among them CUL1 and CUL2, both of which bound to KHNYN in their neddylated forms. Conversely, no significant association was observed with the other constructs. Similar results were obtained for CUL3 and CUL4 (data not shown). Interestingly, CUL1 was precipitated both in the unmodified and NEDD8-conjugated isoform, while only the neddylated form of CUL2 was purified by the NEDD8 GST fusion. This observation is in agreement with reports showing that CUL1, as well as CUL3 and CUL4, forms heterodimers, each dimer composed of one neddylated and one un-neddylated cullin. CUL2 and CUL5, on the other hand, have only been observed as homodimers [31–33]. To exclude the possibility that the interaction of the KHNYN-binding domain with neddylated cullins is mediated by the recognition of ubiquitinated substrates, protein affinity purified with GST-KHNYN from a T-Rex-flag-NEDD8 cell extract were incubated with purified USP8 (ubiquitin-specific protease 8), a deubiquitinating enzyme that specifically removes conjugated ubiquitin and ubiquitin chains from proteins (Fig. 6D). Treatment with USP8 completely removed the poly-ubiquitination signal without affecting the interaction with NEDD8-conjugated substrates. To further confirm that the recognition by KHNYN requires the NEDD8 modification on cullins, we incubated T-Rex-flag-NEDD8 cells with MLN4924, an inhibitor of NEDD8 activation. This approach confirmed that, in the absence of neddylation, CUL2 could not be precipitated by KHNYN (Fig. 6E). Finally, we compared the interaction of KHNYN with ubiquitinated and neddylated substrates after treatment with USP8, the deneddylating enzyme NEDP1 or MLN4924 (Fig. 6F). As shown, the interaction with flag-tagged cellular proteins was similarly disrupted after MLN4924 or NEDP1 treatments (Fig. 6F lanes 6 and 7). Interestingly, the interaction with ubiquitinated substrates was partly affected by the removal of neddylated proteins (lane 7), suggesting that a fraction of ubiquitinated substrates recovered by pull-down are associated with cullin-based complexes. Given the binding properties of the amino acid region spanning the last 52 residues of KHNYN, we have called this novel domain CUBAN, for Cullin-Binding domain Associating with NEDD8.

Structural insights into the binding mechanism of CUBAN to NEDD8

To evaluate the overall folding and secondary structure of the purified CUBAN domain, the circular dichroism (CD) spectrum of the purified protein fragment containing the KHNYN C-terminal 52 amino acids was obtained (Fig. 7A). The fitting of the CD spectrum indicated an α-helical content of 67%, in line with the secondary structure prediction from the Jpred4 server. In order to evaluate the affinity of the CUBAN domain for NEDD8 and ubiquitin, we performed isothermal titration calorimetry (ITC). ITC titration of NEDD8 with the KHNYN domain shows an exothermic binding thermogram (Fig. 7B). The uncertainty in the early steps of the exponential curve allows only rough indications of the binding affinity of the CUBAN domain of KHNYN in complex with NEDD8 that was evaluated to be around 24 ± 2 μM. Finally, NEDD8 A72R mutation causes a reduction in the interaction efficiency (44 ± 7 μM) while binding of KHNYN for ubiquitin was nearly undetectable in these conditions. The pull-down performed with the CUBAN domain incubated with ubiquitin, NEDD8 and the A72R mutant mimicking the C-terminal tail of ubiquitin, confirmed a clear preference of the CUBAN domain of KHNYN for NEDD8 over ubiquitin (Fig. 7C).

Structure in solution of the CUBAN domain

We next determined the solution structure of the CUBAN domain spanning the region from residue 627–678 of the KHNYN-Ct protein. The 52 amino acids in the ^{15}N-labelled protein that were assigned by NMR spectroscopy are indicated using numbering 1–52, as shown in Fig. 8A. To this end, ^{1}H-^{1}H TOCSY,

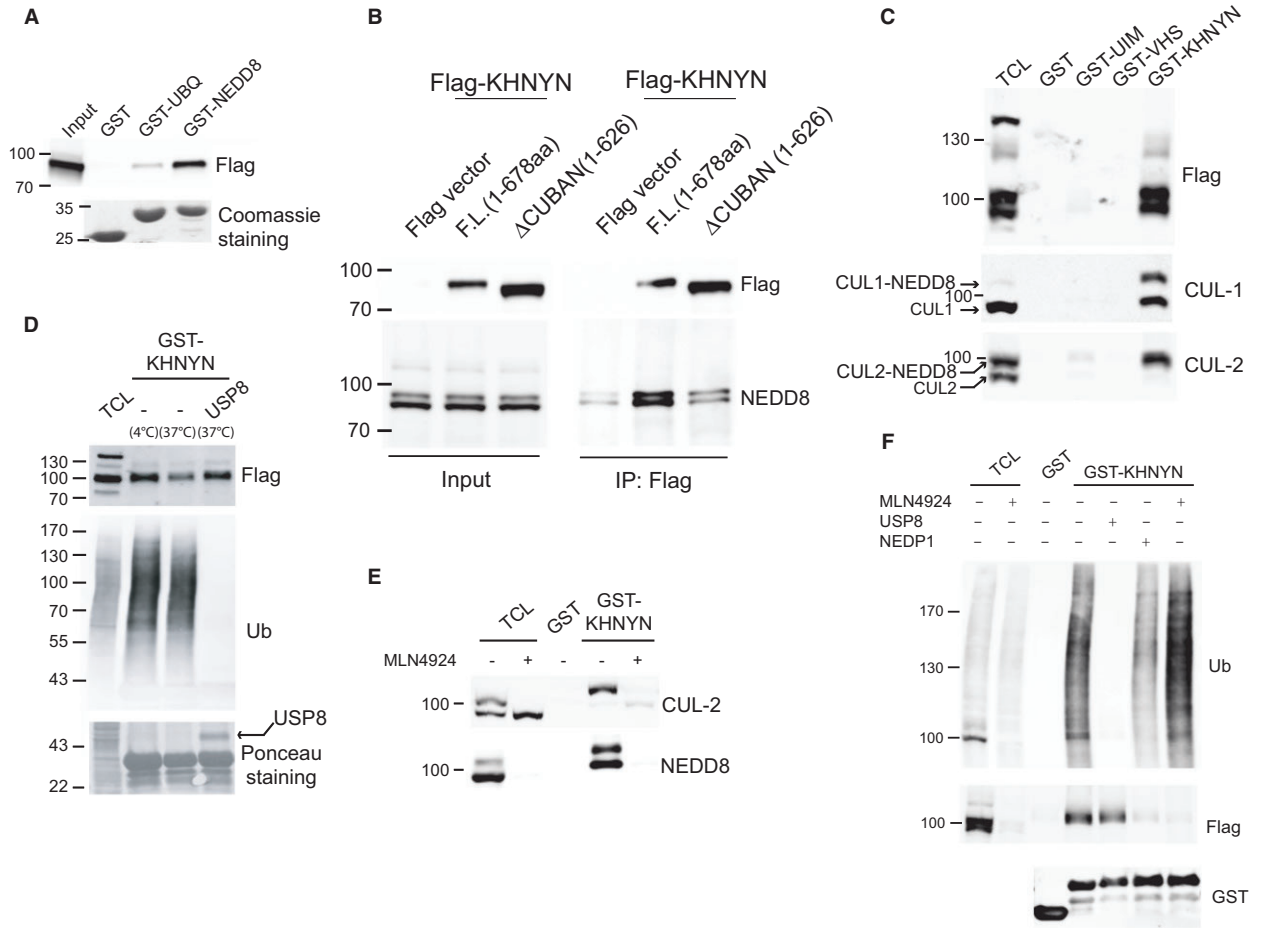

Fig. 6. (A) Full-length KHNYN shows the same binding properties of the isolated domain. HeLa cells were transfected with full-length KHNYN N-terminally tagged with the Flag epitope. Eighteen hours post-transfection cells were lysed and the supernatant incubated with equal amounts of GST, GST-Ubiquitin and GST-NEDD8. After washing, samples were analysed by SDS/PAGE and immunoblotting with anti-Flag antibody. (B) HeLa cells were transfected with the full-length KHNYN (1–678) or with the Delta-CUBAN (ΔCUBAN, 1–626 aa) construct. Eighteen hours post-transfection, cells were lysed and the supernatant immunoprecipitated with anti-Flag antibody. Pellets were analysed by SDS/PAGE and immunoblotting with anti-Flag and anti-NEDD8 antibodies. (C) Neddylated CUL1 and CUL2 associate with KHNYN C-terminal end. The cell lysate from T-Rex flag-NEDD8 cells was used to perform a GST pull-down with KHNYN-Ct, the UIM motif and the VHS domain of STAM2 and with the GST alone. Samples were assayed for the interaction with endogenous neddylated substrates (anti-flag blot) and with CUL1 and CUL2. (D) A fraction of the GST-KHNYN-Ct pull-down from the experiment in (C) was incubated with the deubiquitinating enzyme USP8 for 1.5 h at 37 °C; a similar fraction was incubated at 4 °C or at 37 °C without addition of the deubiquitinating enzyme. After washing, samples were analysed with anti-Flag and anti-Ubiquitin antibodies to monitor the interaction respectively with neddylated and poly-ubiquitinated substrates. (E) T-Rex flag-NEDD8 cells were incubated with MLN4924 1 μM for 3 h or left untreated. The soluble fractions were used to perform a GST pull-down to monitor the interaction of KHNYN-Ct with CUL2. Samples were analysed by SDS/PAGE and immunoblotting with anti-NEDD8 and anti-CUL2 antibody. (F) T-Rex flag-NEDD8 cells were treated as in (E). The soluble fractions of cells treated or untreated with MLN4924 were used in pull-down assay. After washing, samples were incubated with USP8 or NEDP1 and analysed by SDS/PAGE and immunoblotting with anti-Flag and anti-Ubiquitin antibodies to monitor the interaction with neddylated and poly-ubiquitinated substrates.

^{1}H-^{1}H NOESY and ^{15}N HSQC 2D NMR spectra were obtained together with ^{15}N TOCSY-HSQC and ^{15}N NOESY-HSQC 3D spectra using standard methods. The spectra allowed a complete assignment of the resonances. The scalar correlations and the spin systems were identified by TOCSY at different mixing times. After the sequential assignments by the NOESY experiment, the dipolar correlations obtained in the NOESY 2D spectra of the unlabelled protein were used as restraints for molecular dynamics. By the simulated annealing procedure using the CNS software (AALPHA, Information System, Pvt Ltd, Hubballi, India)

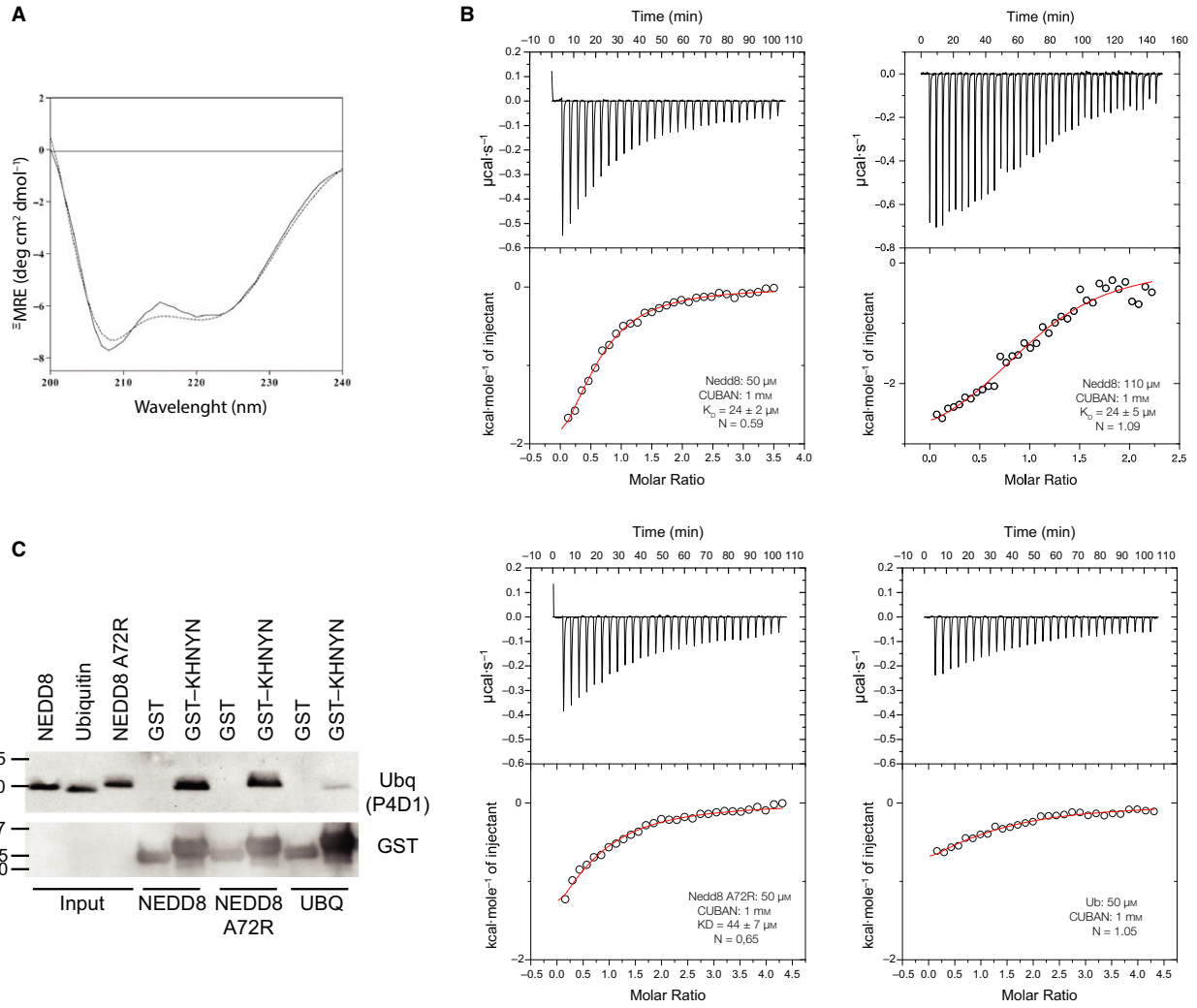

Fig. 7. (A) Circular dichroism spectra of purified KHNYN-Ct. The continuous line represents the CD spectrum of KHNYN, while the dotted line reports the fitting by the algorithms used for deconvolution of spectra. The helix content obtained is the 67%. (B) ITC traces and titration curves of CUBAN binding to NEDD8, NEDD8 A72R and ubiquitin. CUBAN domain at a concentration of 1 mM was injected into 2 mL of solution containing 50 μM of Nedd8 WT, Nedd8 A72R or Ub alone in injection of 4 μL. Two concentrations of NEDD8 (50 and 110 μM) were assayed in independent experiments, obtaining very similar results. (C) The recombinant protein GST-KHNYN-Ct spanning residues 627–678 was incubated with purified Ubiquitin, NEDD8 and the NEDD8 A72R mutant. After washing, samples were analysed by SDS/PAGE and immunoblotting with anti-Ubiquitin antibody from Santa Cruz (P4D1).

the secondary structure elements were obtained as reported in detail in Experimental procedures. Among the 100 structures produced, with backbone atoms RMSD of about 0.7 Å, 12 were selected (Fig. 8B). Structural statistics, detailed description of assigned atoms and the number of short-, medium- and long-range NOEs are reported in Table S1. The top 12 structures resulting were validated by verifying their consistency with the Ramachandran plot using the software PROCHECK (GraficKontrol, Milano, Italy) (see Experimental procedures). In agreement with the CD spectroscopy experiment, NMR spectroscopy revealed a predominantly helical structure (Fig. 6C, left and central panels). While the first five residues were found to be unstructured, the structured part of the molecule (residues 6–52) consists of a three-helix bundle connected by two loops, reminiscent of the typical UBD structure, with the three helices spanning residues T6-R14 (α1), K26-L31 (α2) and Y36-E52 (α3) respectively. Direct inspection of the backbone carbons of the K26-L31 segment identifies a one and a half turn helix-like structure. A peculiarity of the domain is the length and spatial organization of the first loop, spanning residues Q15-H25, with residues V19-F20-W21-G22 in

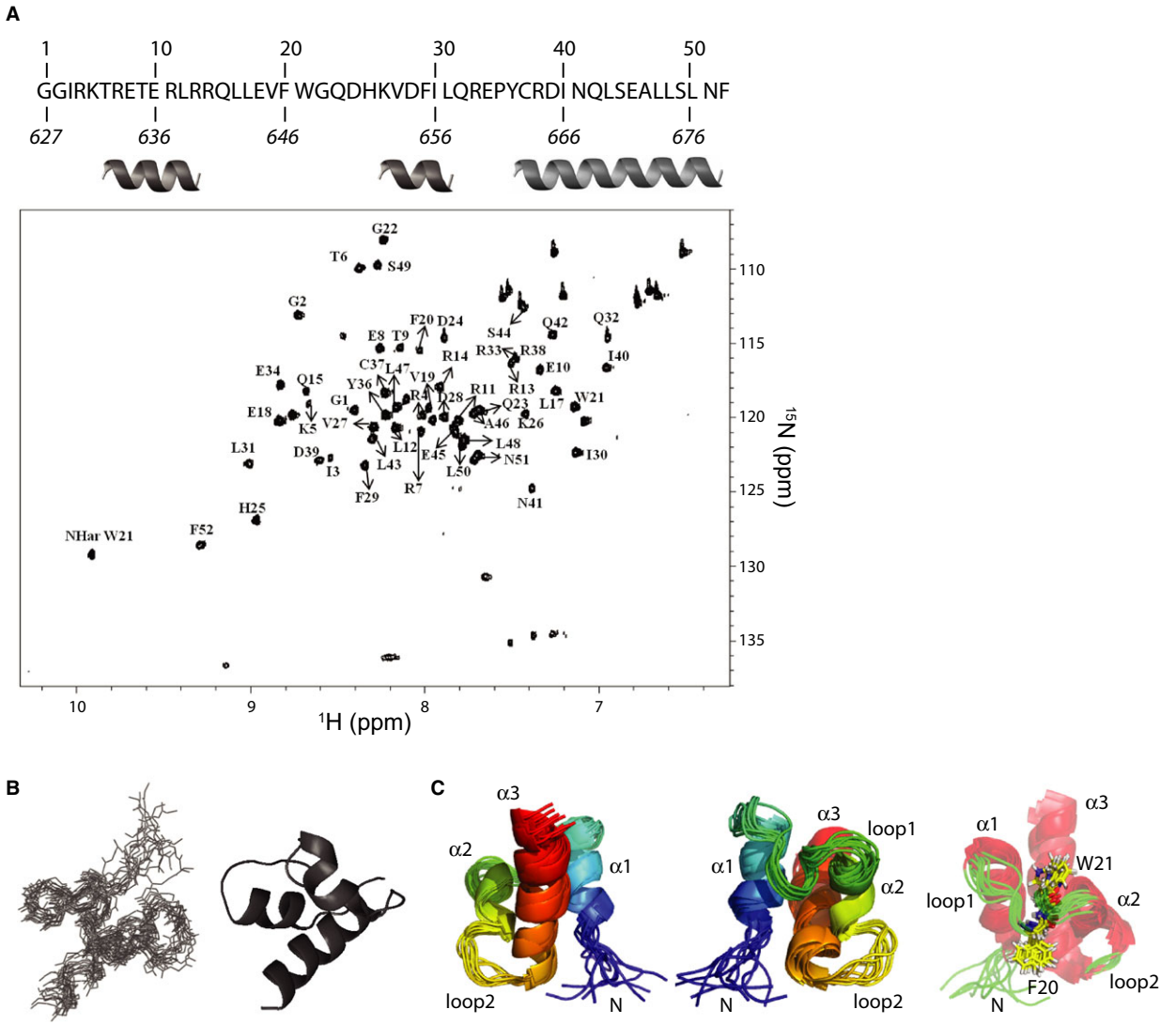

Fig. 8. Structural characterization of the KHNYN-Ct. (A) Assignment of the full ^{15}N HSQC spectrum of KHNYN-Ct obtained by NMR spectroscopy. The sequence of the structured region is shown at the top with the relative numbering here adopted. The numbering of residues referred to the full-length protein is shown in italic at the bottom. (B) Superimposition of the top 12 structures obtained by NMR analysis shows a α-helical organization of the last 52 residues of KHNYN (left). The cartoon representation of one of the top structures is shown (right). (C) Ten lowest energy structures of KHNYN-Ct obtained by CNS 1.3 respecting the NMR experimental restrains (left and central panels). Residues F20 and W21 are in contact with hydrophobic residues of the core and provides a sort of pivot that partially stiffens loop1 (right panel).

the central region of the loop tending to form a helical structure. The φ and ψ angles of most residues in the peptide EVFWGQ are compatible with a helical folding. On the other hand, W21 has φ/ψ values typical of a type-1 beta turn. This feature creates an interruption of the helix after the first two residues (VF). In this conformation, the Phe-Trp pair constitutes a sort of pivot that holds loop1 in a more 'rigid' conformation, thus allowing the two opposite ends connected to helices α1 and α2 to fluctuate and eventually to be involved in protein–protein interactions (Fig. 8C, right panel). Accordingly, molecular dynamic simulations indicate that the linker connecting the Phe-Trp pair to helix α2 shows a marked flexibility and does indeed lack a defined secondary structure in the NMR spectroscopy (data not shown).

Dynamic of the interaction between the CUBAN domain and NEDD8

To ascertain the molecular details of the interaction between the CUBAN domain and NEDD8, we

determined the NMR chemical shift perturbations (CSPs) of the CUBAN domain and NEDD8 spectra upon addition of the unlabelled interaction partner [34]. ^{15}N-labelled CUBAN domain was titrated with unlabelled NEDD8 and similarly ^{15}N-labelled NEDD8 was titrated with unlabelled CUBAN domain. The ^{15}N HSQC of NEDD8 were in close agreement with those deposited in BMRB (entry 10062) and described in literature [35] together with the reported assignments (data not shown). The combined CSPs for the backbone ^{15}N and ^{1}H resonances of both labelled CUBAN (Fig. 9A) and labelled NEDD8 (Fig. 9B) were mapped onto the respective sequences. Regarding the CSPs measurements obtained in the 1 : 1 complex with labelled ^{15}N NEDD8 together with unlabelled CUBAN, 21 residues showed a significant perturbation. Among them, five residues – Val5, Ile13, Glu14, Val30 and Ala72 – showed a perturbation greater than a cut-off of 3σ. In the complementary experiment, we identified four residues in the CUBAN domain, E10, W21, F29 and D39, by using a cut-off of 3σ (9 with a cut-off of 1σ). The docking of the CUBAN domain onto NEDD8 was performed by the HADDOCK (High Ambiguity Driven protein-protein DOCKing) procedure using as constraints the perturbed residues identified in the two separated experiments [34]. Figure 10 reports the structure of the complex between the CUBAN domain and NEDD8 at a molar ratio (1 : 1) in the low-energy cluster obtained by the docking procedure. Among the residues showing a significant perturbation, W21 and F29 in the CUBAN domain highlight a peculiar aspect of this interaction (Fig. 10A,B). While W21 constitutes part of the pivot pointing into the core of the domain, F29 occupies the centre of helix 2 and protrudes out from the protein surface. The CSPs measured for these two residues and mapped on the complex 1 : 1, together with molecular dynamic simulation obtained with GROMACS (Free Software Foundation Europe, Düsseldorf, Germany) (data not shown), suggest that F29 may take part directly in the interaction with NEDD8. Meanwhile, the spatial rearrangement of W21 would suggest a local stiffening of the residues side chains in the region comprised between W21 and F29, that is mainly unstructured in the NMR spectra of CUBAN domain alone. These observations indicate that the side chains in the region between helices-1 and -3, undergo a substantial conformational rearrangement upon binding as reflected by the perturbations on the backbone amide groups ^{15}N resonances. On the other hand, residues 31–34 (EEKE) at the very C-terminal end of the NEDD8 α-helix are found to be part of the contact surface and face the positively charged residues of the CUBAN domain Lys26, Arg33 and Arg38. This indicates the role of polar residues in the interaction, which appears more electrostatic than hydrophobic (Fig. 10C,D), as confirmed by the evidence that the 'canonical' hydrophobic patch seems to be excluded in the interaction between the two partners (Fig. 10E,F). The structure obtained for the CUBAN domain of KHNYN (597–678) and for the complex with NEDD8 has been deposited in the PDB with label 2N5M the former and 2N7K the latter. The complete assignments of NMR resonances have been deposited in BMRB data bank with labels 25722 and 25808 respectively (Fig. 11A). It should be pointed out that the structure of the CUBAN domain alone (with a good RMSD in the MD simulation) is to be considered a good HADDOCK model more that a precise solution structure. More detailed information obtainable by other NMR techniques, such as residual dipolar coupling, would be impossible to achieve due to the tendency of the CUBAN domain to precipitate during measures, a process that is most likely accelerated in an orienting medium.

To confirm our model, we mutated residues Glu31 and Glu32 in NEDD8 by substituting them with the corresponding residues in ubiquitin (Glu31Gln and Glu32Asp) or with an opposite charge (Glu31Lys and Glu32Lys). These mutants, together with the Ile44Ala and the Ala72Arg mutants, were assayed in a pull-down experiment against the purified CUBAN domain (Fig. 11B). As shown, there is a clear loss of binding when mutating the hydrophobic patch key residue Ile44, while the Ala72Arg mutation reduces the binding efficiency as previously shown. In addition, there is a reduction in binding efficiency when using the mutants H25F and R38E, but not K26D and R33E, in the electrostatic binding surface of CUBAN domain (Fig. 11C). Moreover, the two mutants W21A and W21P were also assayed in this experiment in order to evaluate the function of this residue in the interaction. Interestingly, both mutants show a partial reduction in binding efficiency, with the mutation in Pro being more effective that the Ala substitution. Together with F20, the W21 constitutes the above-described pivot, which affects the loop1's degree of flexibility. Upon binding with NEDD8, the flexibility of the region comprised between W21 and F29 is reduced, as shown by NMR. Therefore, the differences observed in the two mutants W21A and W21P are likely the result of two opposite effects: while the W/A substitution increases the stiffness of the pivot, a destructuration phenomenon is expected for the W/P substitution, leading to an increase in the flexibility in the entire loop region.

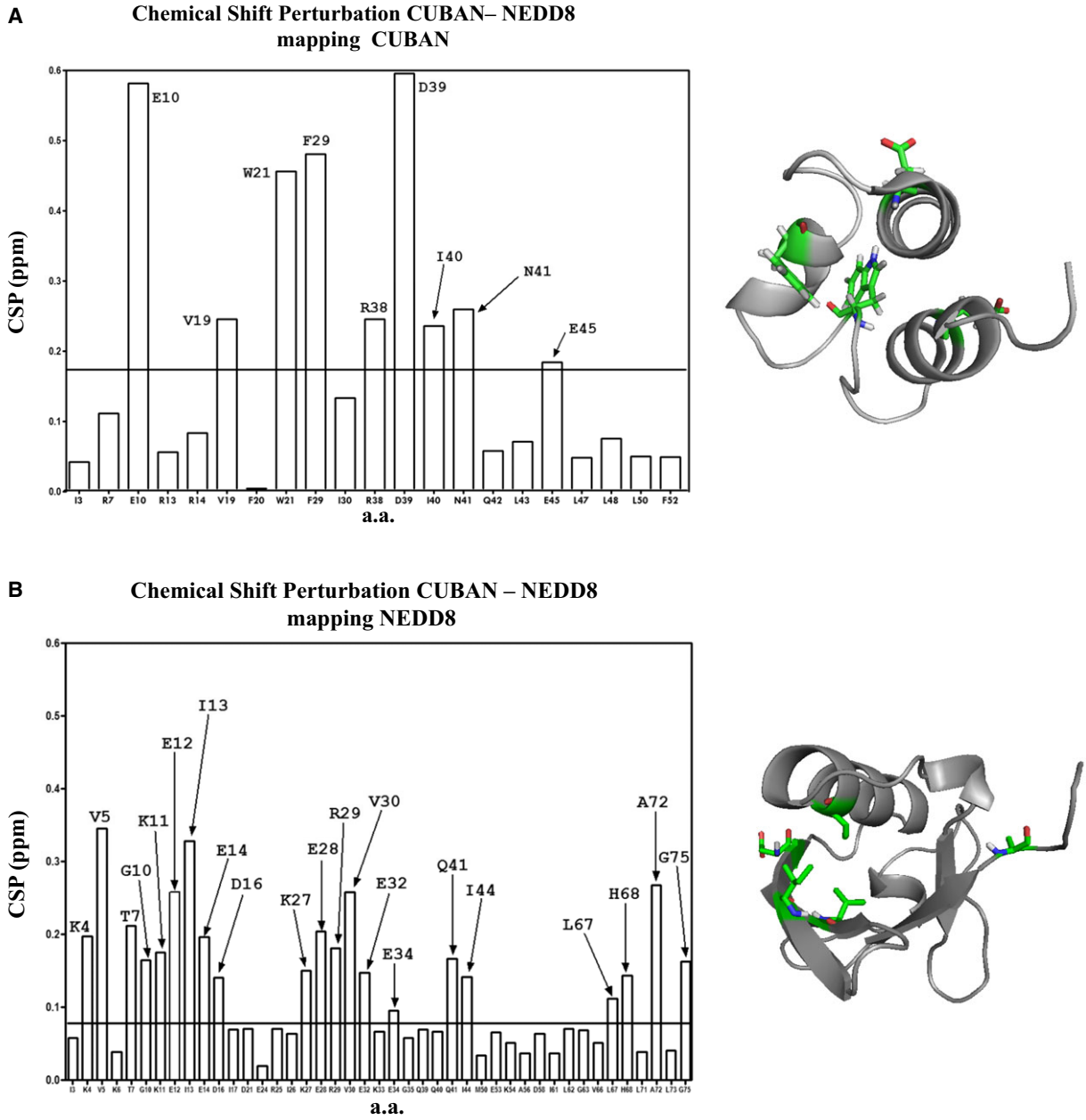

Fig. 9. Structural characterization of the CUBAN domain in complex with NEDD8. (A) Combined CSPs for the backbone ^{15}N and ^{1}H resonances of labelled NEDD8 in the presence of KHNYN to a molar ratio 1 : 1 (B) and labelled KHNYN in the presence of NEDD8 to a molar ratio 1 : 1. The continuous line indicates the chemical shift change used as a threshold value. Residues showing a perturbation greater than a cut-off of 3σ are shown in the ribbon representation. Only residues showing a detectable CSP are shown. The secondary structures of CUBAN and NEDD8 are shown.

The surface representation of CUBAN/NEDD8 complex is shown in Fig. 12A, together with a magnification of the region surrounding Ala72 of NEDD8. This residue maps in the C-terminal tail of the molecule, which is extremely flexible. In fact, these regions are very rarely characterized by NMR, making it rather difficult to rationalize them in terms of structural properties and thus requiring caution in the interpretation of any conclusion concerning the effect of mutations. That said, by inspecting the spatial organization of Ala72 with respect to the residues involved in the interaction between the two molecules, we can

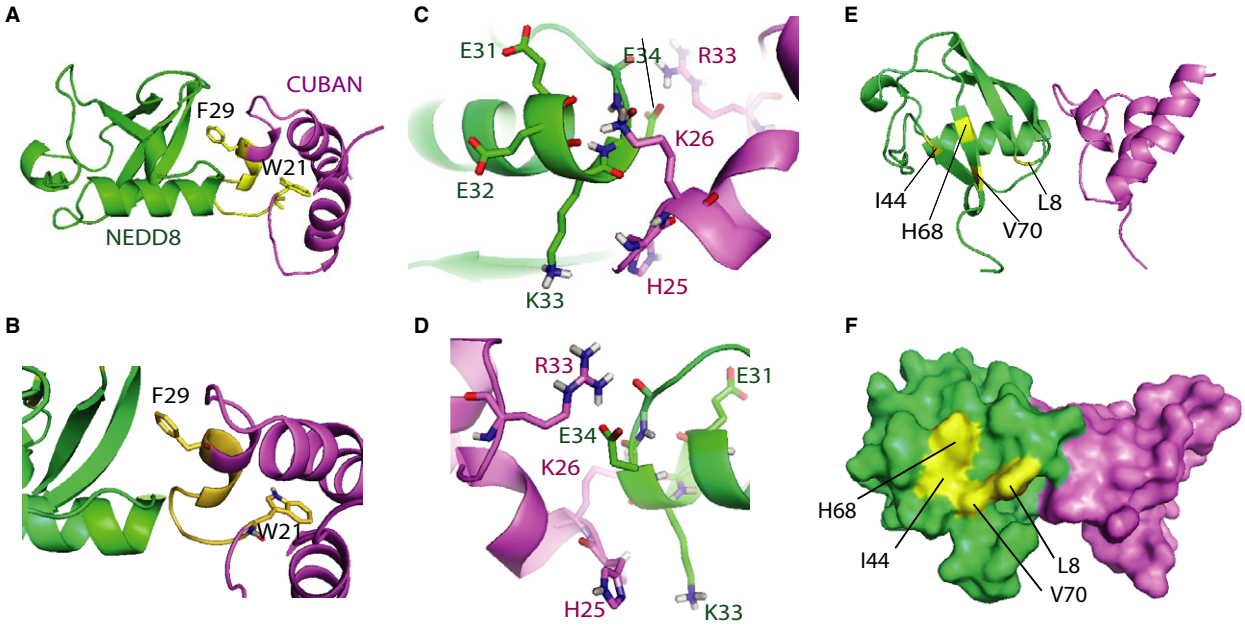

Fig. 10. Identification of the binding surfaces involved in the recognition of NEDD8 by the CUBAN domain. (A, B) Ribbon representation of the KHNYN C-terminal domain (violet) in complex with NEDD8 (green). The KHNYN structure is partially shown to highlight the spatial organization of W21 and F29. The backbone chain including the region between W21 and F29 (green) shows a very high mobility with residues G22-H25 presenting no defined secondary structure. Panel B shows a magnification of the section presenting described in A. (C, D) Ribbon and surface representations of the KHNYN C-terminal domain (violet) in complex with NEDD8 (green) showing the residues defining the Ile44-centred hydrophobic patch (yellow). (E, F) Spatial organization of the 31-EEKE-34 sequence in NEDD8 (green) and of the positively charged surface in KHNYN C-terminal domain (violet) including residues H25, K26 and R33. Panels show two images rotated 180 degrees.

speculate on how the substitution Ala72Arg could affect the recognition between CUBAN and NEDD8. Indeed, four charged amino acids, Arg33 and Arg38 in CUBAN and Glu31 and Glu32 in NEDD8, surround at different distances the flexible C-terminal tale of NEDD8 (Fig. 12B). We can suggest that the presence of an arginine in place of the alanine would cause transient electrostatic interactions between polar or dipolar nearby side chains. For example, an electrostatic repulsion with the arginines in CUBAN and/or a polar interaction with Glu residues in NEDD8 could affect the extension and strength of the binding surface.

We finally asked whether the interaction of the CUBAN domain with ubiquitin chains could compete with NEDD8's binding. To this end, we performed a pull-down experiment in which the GST-CUBAN fusion was incubated, in the presence of NEDD8, with increasing concentrations of diubiquitin chains, both the linear, having an open conformation (Fig. 13A), and the K48-linked type that is typically characterized by a compact conformation in which the distal (linked via its C terminus) and the proximal (linked via its Lys residue) ubiquitin moieties form an intramolecular interface (Fig. 13B) [36]. Both diubiquitin chains compete with NEDD8's binding, ending with the complete displacement of the Ubl. Based on our preliminary data, we observe a stronger interaction with K48-linked chains. Moreover, in both competition assays, the interaction of CUBAN with NEDD8 seems to be strengthened in the presence of 1 μM Ub2, particularly in the case of K48 chains, after which it gradually declines. Even though these observations require further validations, one could argue that the flexibility of CUBAN domain allows KHNYN to participate to protein complexes where both neddylated and ubiquitinated substrates are involved, at least within fixed molar ratios, so that the overall conformation is significantly affected by KHNYN-binding partners. In this regard, the simplified condition involving only the last 52 amino acids of CUBAN and the shortest ubiquitin chains is sufficient to demonstrate that the addition of diubiquitins to the CUBAN/NEDD8 complex directly causes a conformational change in CUBAN associated with a change in NEDD8 binding affinity. Given that the effect is caused by the addition of ubiquitins in

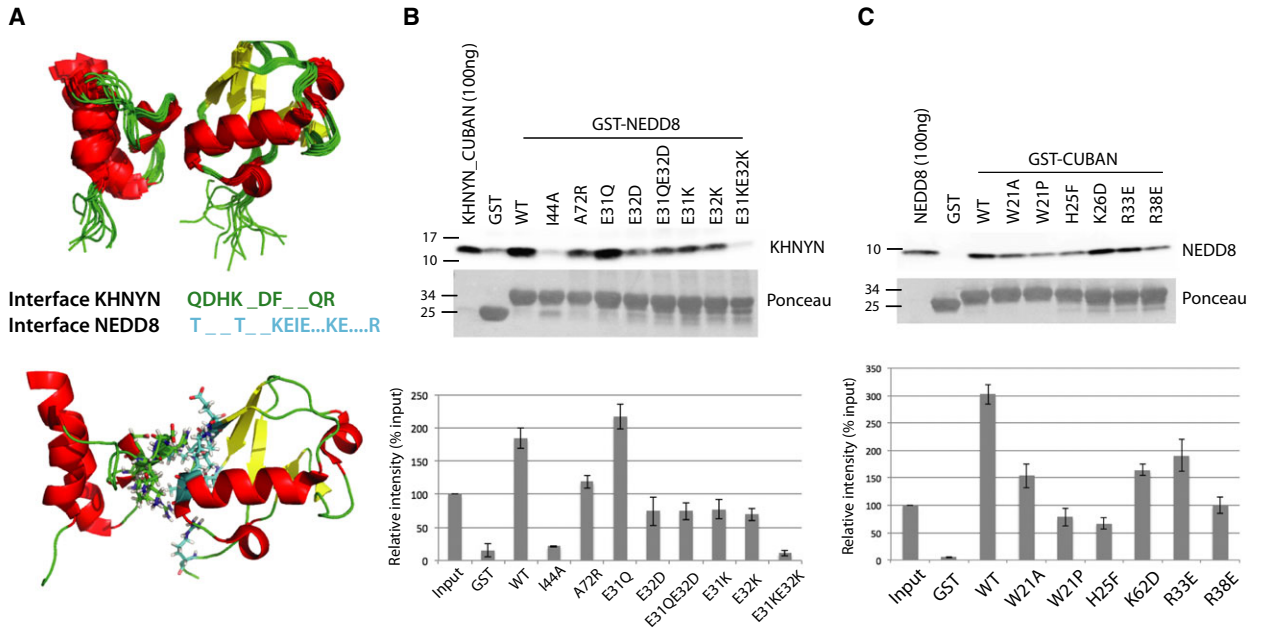

Fig. 11. (A) Cartoon representation of CUBAN/NEDD8 structures obtained by HADDOCK 2.0 (upper panel). Residues are shown respectively in green (KHNYN) and cyan (NEDD8) colours ball and stick models (lower panel). Residues involved in the interacting surfaces are shown. (B) Functional analysis of mutations affecting the NEDD8- and CUBAN-binding sites. Residues E31 and E32 in NEDD8, fused to the GST, were mutated in the corresponding positions in ubiquitin (E31Q, E32D) or in lysines (E31K, E32K). These mutants, together with I44A and A72R NEDD8 mutants, were assayed by pull-down versus the purified CUBAN domain. The interaction was revealed by western blotting with the anti-KHNYN antibody. Densitometry calculations of bands were made using IMAGEJ software and signals were expressed as percentage of the input intensity. (C) The point mutations W21A and W21P, H25F, K26D, R33E and R38E (with numbering corresponding respectively to positions W647, H651, K652, R659 and R664 in the full-length protein) were inserted in the GST-CUBAN recombinant protein and assayed by pull-down against monomeric NEDD8. The interaction was revealed by western blotting with the anti-NEDD8 antibody. Densitometry calculations of bands were made using IMAGEJ software and signals were expressed as percentage of the input intensity. Data are shown as mean ± SD.

chain, the displacement of NEDD8 could be the result of both a conformational effect and the steric hindrance of the diubiquitins. Obviously, we can predict that regulatory mechanisms must account for the variability and selectivity of KHNYN binding properties at physiological conditions.

Discussion

Ubiquitination of eukaryotic proteins is a signalling event that, since its first description, recalls today much more biological processes than that was originally thought. The presence of up to 16 different ubiquitin-like peptides, which can be covalently linked to a variety of proteins, adds further complexity by widening the spectrum of cellular processes regulated by Ub/Ubl conjugation. At the same time, however, the balance between specificity and promiscuity in these modifications becomes particularly relevant. The case of ubiquitin and NEDD8 is particularly intriguing. Despite the high level of similarity, the two post-translational modifications target a very different number of substrates. While a few proteins are stably neddylated, many proteins are regulated by ubiquitination. Strikingly, alongside a clear biological function of neddylation, ubiquitin-binding domains are in general rather promiscuous and bind to either modifications although not necessarily with similar efficiency. Moreover, as also shown here, only a few domains are selective for ubiquitin while no domain that specifically binds NEDD8 has been reported to date.

Based on these premises, we carried out an unbiased search of ubiquitin- and NEDD8-binding domains by panning a cDNA fragments library, displayed on the bacteriophage lambda, to investigate their specificity and promiscuity. When the selected domains were assayed for their interaction with the NEDD8 mutant bringing the substitution Ala72Arg, the UBD of KHNYN resulted to be the only one whose interaction with NEDD8 was affected by the acquisition of ubiquitin features in the C-terminal tail of the molecule.

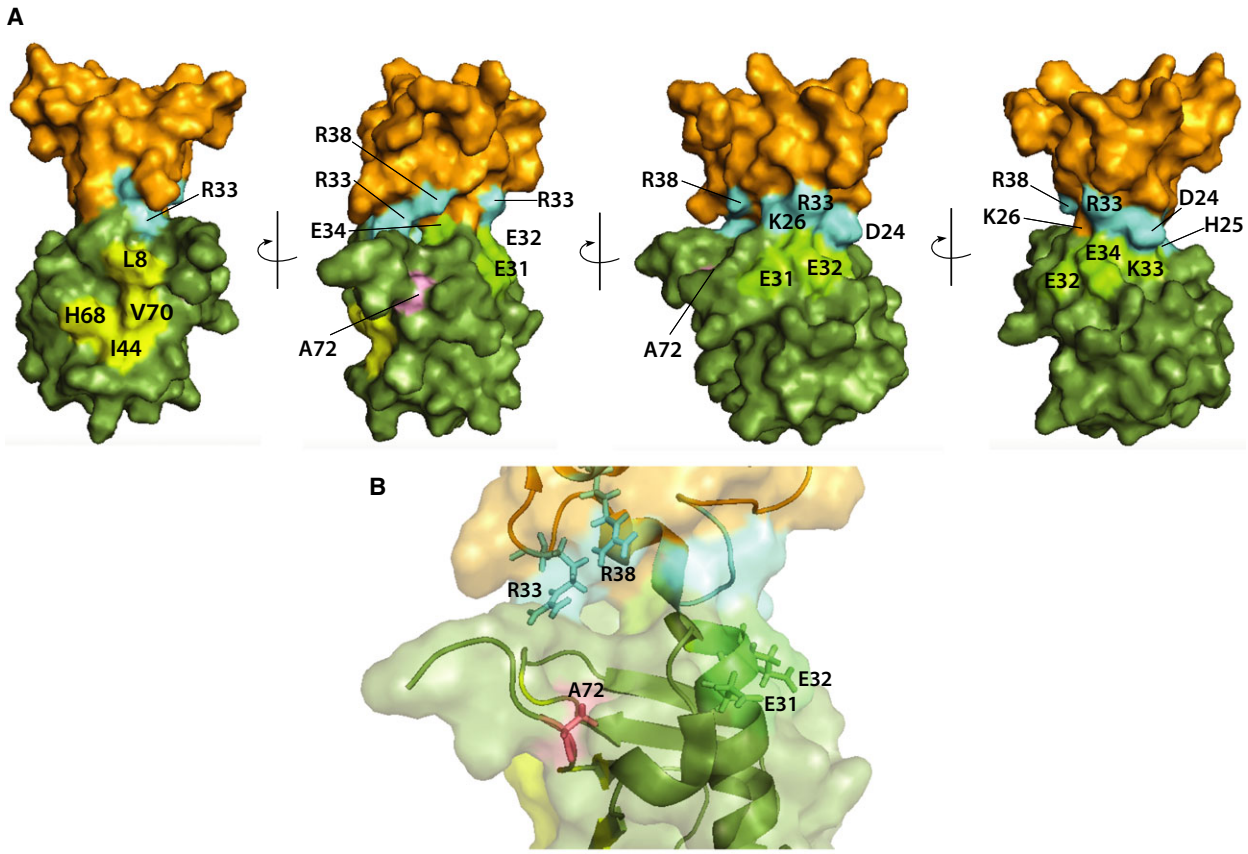

Fig. 12. (A) The molecular surface representation of CUBAN in complex with NEDD8 is shown with NEDD8 coloured orange, the hydrophobic patch yellow, the A72 residue pink, the CUBAN contact surface lime, the CUBAN domain orange and the NEDD8 contact site cyan. Each complex is rotated about 45 degrees from the vertical axis. The positively charged surface in the CUBAN domain packs against the negative patch of NEDD8. (B) Magnification showing residues A72, E31, E32 of NEDD8 and R33 and R38 in CUBAN. Side chains are represented in sticks.

The NEDD8 binding region identified in KHNYN maps to the carboxyl-terminal end and shows both the features of a stronger binding towards NEDD8 versus monomeric ubiquitin and the capability of interacting with neddylated cullins. Based on these properties, we dubbed the region spanning the C-terminal 52 residues of KHNYN the CUBAN domain, for Cullin-binding domain Associating with NEDD8. The first relevant point emerging from our analysis is that the CUBAN domain, although clearly preferring monomeric NEDD8 to ubiquitin recognizes both molecules and therefore cannot be considered specific. Nevertheless, we are able to state that the CUBAN domain is selective for NEDD8 since it has evolutionary gained a recognition mode of NEDD8 that cannot be mimicked by ubiquitin. Accordingly, KHNYN was selected also as an ubiquitin-binding domain-containing protein and the interaction with endogenous poly-ubiquitinated substrates suggests that binding efficiency is favoured when ubiquitin moieties are conjugated to form polymeric chains. This assumption is confirmed by our *in vitro* competition assays (Fig. 13A,B) showing that diubiquitin chains, both linear and K48-linked, replace the interaction between CUBAN and NEDD8, most likely because the contact sites required for the association with ubiquitin chains partially overlap with the NEDD8-binding site.

To understand the molecular basis of NEDD8 recognition, we determined the structure in solution of this novel domain and we characterized the interaction surfaces between the CUBAN domain and NEDD8 by NMR spectroscopy, mutagenesis, model docking and molecular dynamics. Among the large variety of ubiquitin-binding domains described to date, the CUBAN domain shows structural elements that are common in other UBDs, first of all belonging to the most populated category represented by a three-bundle helix [37] (Fig. 8). By comparing the CUBAN with members of

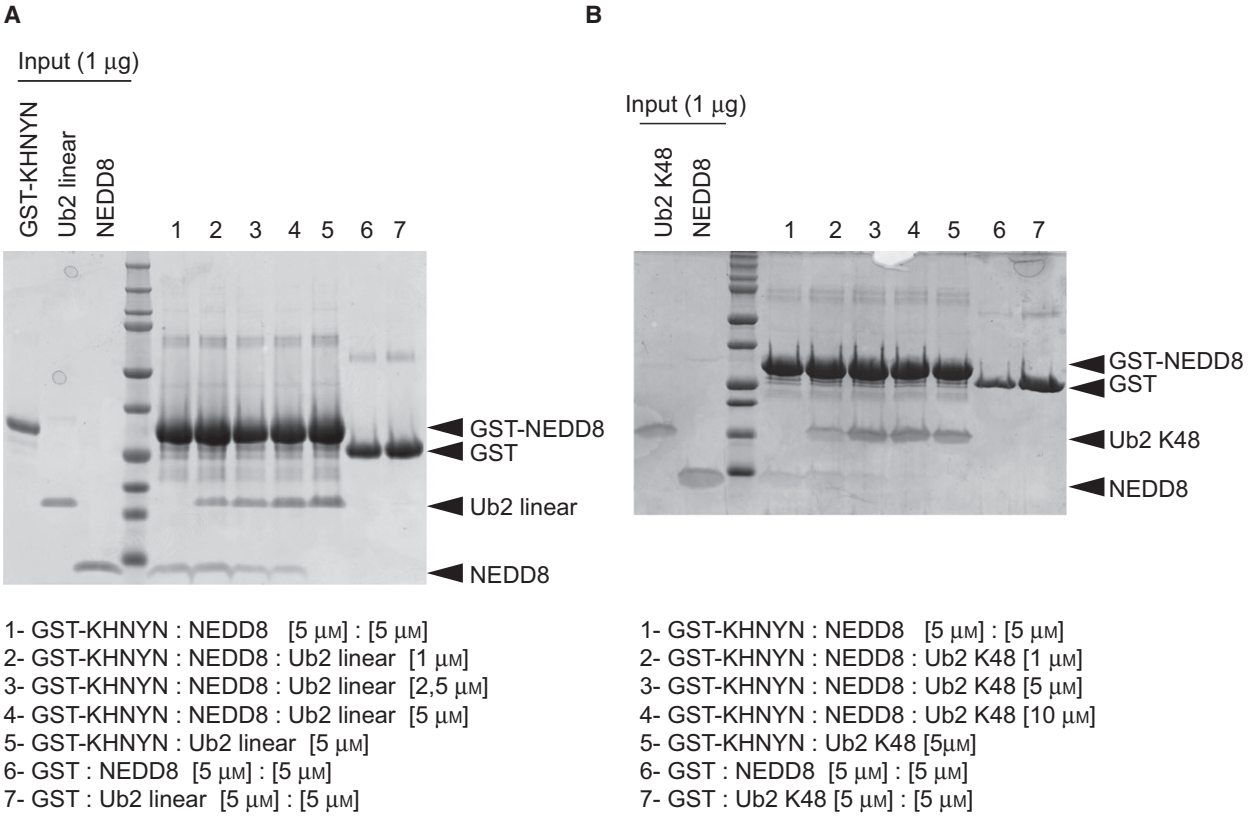

Fig. 13. (A, B) The interaction of the CUBAN domain fused to the GST with monomeric NEDD8 is disrupted by the addition of increasing amount of diubiquitin chains, both linear and K48-linked type, as shown in the figure (lanes 1–4 in both panels). The interaction of KHNYN with the diubiquitin chains in the absence of NEDD8 is also shown (lane 5). Lanes 6 and 7 represent the control experiment performed with the GST alone. The concentration of bait and preys for each tested condition is indicated in figure.

the UBA (PDB 1V92) and CUE family (PDB 2EJS), we observed that the second helix in the CUBAN structure is located on the opposite side of the plane passing through helices 1 and 3 (Fig. 14A). This observation suggests that the CUBAN represents a structural variant of three-bundle helix domain, showing a functional convergence regarding the recognition of ubiquitin and the unique feature of recognizing NEDD8. The 1 : 1 complex determined by NMR spectroscopy using as restraints the CSPs of the labelled-unlabelled proteins, indicated that the CUBAN domain binds to residues in the second β-strand (Ile13 and Glu14) and in the C-terminal end of helix α-1 (Glu31-Glu34) of NEDD8 (Figs 10 and 11). Moreover, the contact interface in the CUBAN domain shows residues with highly flexible side chains, thus suggesting that the conformation of the domain within the complex structure could be eventually determined by NEDD8 itself. The interacting surface in NEDD8 shows negatively charged residues (31-EEKE-34) contacting a positively charged surface in the CUBAN domain including turn1, helix α2 and turn2. The binding interface is essentially different in NEDD8 when compared to ubiquitin. Indeed, most of the Glu residues in NEDD8 are replaced by polar residues (Thr, Gln) or with Asp, having a shorter side chain than the very similar glutamate in ubiquitin (Fig. 14B). Thus, subtle side chain differences between NEDD8 and ubiquitin could explain how the Ubl dictates the specificity. Interestingly, the molecular details of this interaction are reminiscent of the electrostatic interaction between the acidic residues Glu31 and Glu32 in NEDD8 and the linker of RBX1, allowing the enzyme to acquire a conformation that is functional for the neddylation of CUL1 [38].

Obviously, other elements may impact on the structure and the dynamic of this complex: firstly, when conjugated to cullins, NEDD8 shows an accessibility that is different from the monomeric state. Moreover, cullins themselves could directly or indirectly play a role in the interaction, for example, by introducing conformational changes, dimerization and eventually

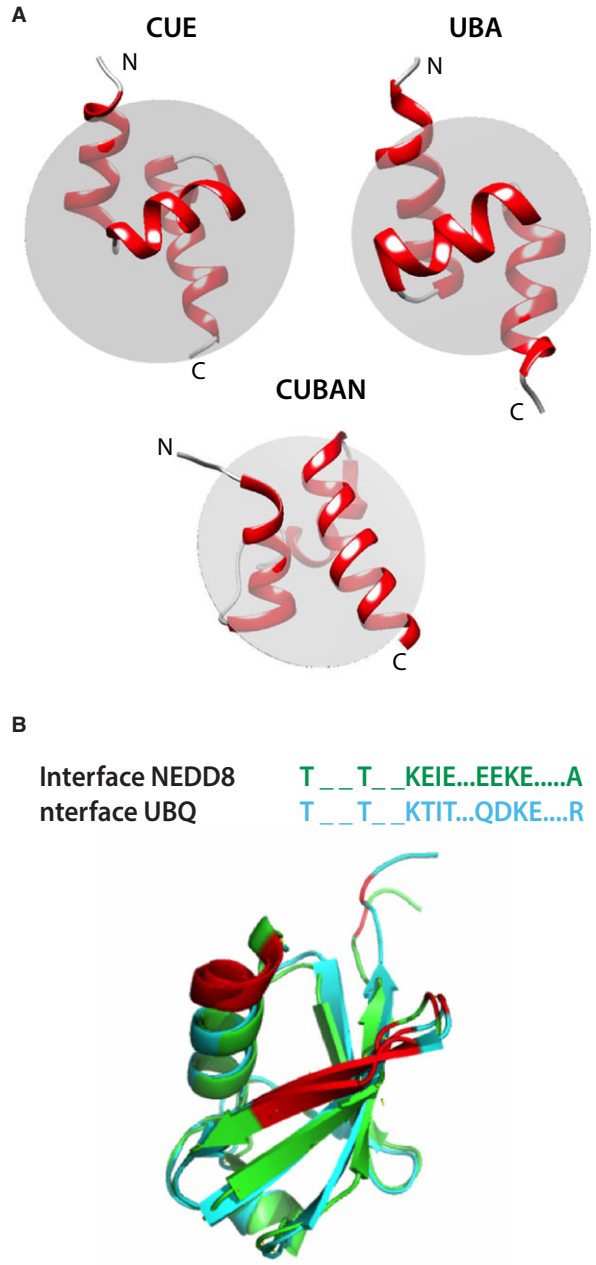

Fig. 14. (A) Ribbon representation of CUE (PDB: 2EJS), UBA (PDB: 1V92) and CUBAN (PDB: 2N5M) domains. (B) Superposition of NEDD8 (green) and ubiquitin (cyan). The molecular determinants for distinguishing between ubiquitin and NEDD8 by the CUBAN domain are shown in red and in the sequence alignment.

allosteric rearrangements that could affect the definitive complex structure. In the same way, other regions in the full-length KHNYN could provide structural features involved in determining the recognition and the discrimination between ubiquitin and NEDD8. Last but not least, the region of KHNYN selected by our screening included the last 81 residues of the amino acidic chain. One of the advantages of the phage display approach is that bacteriophages displaying partially overlapping regions of the same protein, are enriched in proportion to the binding efficiency of each fragment towards the same GST fusion. Therefore, the clone that, at the end of the last round of selection, turns out to be the most represented generally includes the optimal bait-binding region. Based on this assumption, the resolution of the structure containing the full range of residues selected in our screening could provide further details to the present analysis.

A second essential point emerging from our analysis is that the CUBAN domain also binds endogenous poly-ubiquitinated substrates and that diubiquitin chains are able to replace the interaction with NEDD8 at least at determined molar ratios, suggesting that the recognition of both molecules by the CUBAN domain is basically mutually exclusive. On one hand, the observation that the CUBAN domain does not interact with Ub monomers but efficiently recognizes Ub chains, confirms the typical binding properties of physiological Ub–UBD interactions, that are mediated by multivalent contact sites [39]. On the other hand, the CUBAN domain shows a binding affinity for monomeric NEDD8 that has been evaluated to be around 24 μM, a measure that is comparable to the highest affinity for ubiquitin observed for some CUE and UBA domains [37]. This property could guarantee the interaction with mono-neddylated substrates but not with those that are mono-ubiquitinated. If we consider that the concentrations of free ubiquitin and NEDD8 were reported to be roughly equimolar [26] and that in the experimental conditions in which we detect the interaction with endogenous monomeric NEDD8, the interaction with free Ub is undetectable, we can affirm that the CUBAN domain selectively recognizes NEDD8, both as a monomer or conjugated to cullins. Moreover, in the absence of poly-ubiquitin chains, the interaction with NEDD8 and neddylated substrates is favoured and this is achieved via a dedicated binding site whose accessibility is presumably regulated by other protein–protein interactions. The presence of a selective NEDD8-binding site supports the notion that the CUBAN domain is able to distinguish between Ub and the Ubl, thus excluding any form of promiscuity.

On a speculative plane, the CUBAN could also recognize mixed Ub-NEDD8 chains that are conjugated to many proteins under stress conditions, such as the depletion of free ubiquitin induced by different drugs, or in cancer cells where NEDD8 and the neddylating enzymes are overexpressed. If this actually happens, it would further support the notion that KHNYN

function could reveal insights into the cross talk between different Ubl pathways in specific cellular conditions.

Hardly any information is available regarding the biological function of KHNYN. The primary sequence contains an N-terminal evolutionary conserved KH domain (K Homology), first identified in the human heterogeneous nuclear ribonucleoprotein (hnRNP) [40], that is present in a wide variety of nucleic acid-binding proteins where it binds RNA and can function in RNA recognition [41]. Following the KH domain, there is the NYN domain (N4BP1, YacP Nucleases) with predicted ribonuclease activity, which is found in the eukaryotic proteins typified by the NEDD4-binding protein 1 and the bacterial YacP-like proteins [27]. From this perspective, the discovery that the C-terminal region of KHNYN engages an interaction with cullin-RING ubiquitin ligases is extremely attractive, since it unmasks an unsuspected connection between RNA metabolism and proteins and complexes regulated by neddylation.

Experimental procedures

Antibodies and reagents

Monoclonal anti-flag (M2-Affinity Gel) and polyclonal anti-flag were from Sigma (St Louis, MO, USA), anti-tubulin and anti-ubiquitin P4D1 from Santa Cruz Biotechnology (Santa Cruz, CA, USA), anti-NEDD8 was from Abcam (Boston, MA, USA), anti-rabbit and anti-mouse peroxidase-conjugated were from Jackson Immunoresearch (West Grove, PA, USA). Diubiquitin chains were from UBPBio (Aurora, CO, USA).

Plasmid construction and site-directed mutagenesis

The human *KHNYN* gene (NM_015299) was cloned into the pcDNA3.1 vector using primers R1613 CCGAATTC ATGCCTACCTGGGGGGCCCGC (forward) and R1614 CCGCGGCCGCTATCAAAAGTTAAGACTGAGCA (reverse). The human *NEDD8* gene (NM_006156), fused to the flag epitope at the N-terminal end, was cloned into the pcDNA FRT/TO vector (Invitrogen, Frederick, MD, USA). Prof. Vjekoslav Tomaić kindly provided the plasmid for the expression of the GST-S5a construct. The T-Rex flag-NEDD8 cell line was generated according to the manufacturer's instructions. Chimeric constructs were generated by synthesizing partially overlapping PCR fragments subsequently annealed and inserted into pGEX2TK (GE Healthcare, Chicago, IL, USA). Site-directed mutagenesis of NEDD8 I44A, A72R, E31Q, E32Q, E31QE32D, E31K, E32K, E31KE32K and CUBAN W21A, W21P, H25F, K26D, R33E and R38E were performed using the QuikChange® Site-Directed Mutagenesis Kit (Invitrogen) according to the manufacturer's instructions.

Selection of recombinant lambda phage particles

Human ubiquitin and NEDD8 were expressed in bacteria as GST fusion proteins, immobilized on glutathione-Sepharose 4B beads (Amersham Pharmacia Biotech, Little Chalfont, UK) and used as baits for affinity selection of interacting clones from a human brain cDNA library whose products are displayed on the surface of the lambda capsid [42]. The library is formed by 10^8 independent cDNA clones expressed by fusion to the carboxyl end of the D capsid protein. After a preincubation of 4 h in PBS containing 3% (w/v) BSA at 4 °C, 50 μg of the bait fusion protein immobilized on Sepharose beads were incubated 2 h at 4 °C with 0.2 mL of brain cDNA library (corresponding to 3×10^{10} recombinant particles) in dilution buffer (150 mM NaCl, 10 mM MgSO4, 35 mM Tris-HCl, pH 7.5). The Sepharose beads were collected by centrifugation and washed five times with 1 mL of ice-cold PBS/Tween-20 (0.05%, v/v). Unbound particles were conserved for titration. Selected phages were recovered by adding to the washed resin 1 mL of fresh BB4 bacteria (A600 nm = 0.5) grown in LB medium containing 0.2% (w/v) maltose and 10 mM MgSO4. At each panning cycle we monitored the enrichment of binding clones by determining the ratio between the total number of phages loaded onto the affinity column and the number of adsorbed phages (N/A ratio) and by analysing by PCR the pool of phages collected at each round of panning (Fig. 1). Phages obtained after the final round of selection were plated on agar plates, and clones were randomly selected for DNA isolation. Lambda plaques were isolated and eluted in 50 μL of SM buffer and 2 μL of chloroform. A 1 μL sample was then utilized for PCR reaction using primers R324 5′-ATGTATCAGTGCCTAGC-3′ and R325 5′-CACGTTCCGTTATGAGGATGT-3′. The sequences of cDNA products displayed on phage clones were determined by automatic sequencing (ABI PRISM 310 Perkin Elmer, Waltham, MA, USA) of phage single-stranded DNA using universal primers. We considered for further analysis clones encoding (a) different partially overlapping fragments of the same protein and (b) clones predicting the synthesis of protein domains matching the consensus of already characterized ubiquitin-binding domain families. Clones containing repeated Alu sequences or coding sequences that were not in frame with the lambda D protein were excluded from further characterization.

Subcloning of the cDNA fragments selected by ubiquitin and NEDD8

The cDNA fragments contained in the affinity-selected recombinant particles were cloned into the pGEX2TK

expression vector (Amersham Pharmacia Biotech) in frame with the GST coding sequence, using primer R2159 GTTGGATCCGCAATCAGCATCGTTACG (forward) and primer R1542 GTTGAATTCTCAAAAGTTAAGACTGAG (reverse). The cDNA fragments were subcloned in pEGFP-C1 for the transient expression in eukaryotic cells, using primers R2134 TCAGATCTGCAATCAGCATCG TTA (forward) and R2136 CGTGGATCCTTACTTAGC GGCCGC (reverse).

Expression plasmids and protein purification

The cDNA fragments contained in the affinity-selection recombinant particles were cloned in pGex2TK vector for bacterial expression. GST fusion proteins were prepared as previously described [43]. The amino acid region spanning residues 627–678 of KHNYN was cloned in the pGex2T vector (Amersham). The recombinant protein was expressed in BL21 bacterial cells according to the protocol for NMR sample preparation described by Weber *et al.* [44].

Pull-down assays

For the pull-down experiments, equimolar amounts of GST fusion proteins corresponding to the selected clones and GST alone, linked to glutathione-Sepharose 4B beads, were incubated 1.5 h with 1 mg of T-Rex-flag-NEDD8 cells lysed in 25 mM Tris pH 7.5, 125 mM NaCl, 1% glycerol, 1 mM $MgCl_2$, 1 mM orthovanadate, 5 mM NaF, 0.5% Triton-X100, 0.5% NP-40, proteases inhibitor cocktail (Sigma). Beads were washed three times in washing buffer (25 mM Tris pH 7.5, 125 mM NaCl, 1% glycerol, 1 mM MgCl2, 1 mM orthovanadate, 5 mM NaF, 0.5% NP-40, proteases inhibitor cocktail) and bound proteins were electrophoresed on polyacrylamide gel, transferred to PVDF or nitrocellulose membranes, and detected with specific antibodies. For the coimmunoprecipitation assay HeLa cells were plated in 100-mm dishes and grown to 60–70% confluence in culture medium supplemented with 10% FBS. Twenty hours post-transfection cells were solubilized in lysis buffer. An equal amount of each protein lysate was incubated with anti-Flag M2 affinity gel beads for 2 h at 4 °C and then washed three times with washing buffer supplemented with fresh inhibitors. The protein lysates and the immune complexes were analysed by western blot analyses with rabbit anti-Flag and anti-NEDD8 antibodies.

Competition assay

For the competition assays shown in Fig. 11, equimolar amounts (5 μM each) of purified proteins GST-KHNYN and Nedd8 were incubated for 2 h at 4 °C with an increasing amount (from 1 to 10 μM) of Ub dimer either linear or K48 linked. GST alone (5 μM) was incubated with an equimolar amount of Nedd8 or Ub dimers as negative control. After incubation, beads were washed three times with YY buffer (50 mM Hepes pH 7.5, 10% glycerol, 150 mM NaCl, 1% Triton X-100, 1 mM EDTA, 1 mM EGTA) and specifically bound proteins were resolved with Tris-Tricine PAGE (11%) followed by staining with Coomassie blue.

Isothermal titration calorimetry

Isothermal titration calorimetry measurements were performed on a MicroCal VP-ITC (Microcal LCC, Northampton, MA, USA) instrument at 24 °C. All proteins were extensively dialysed against ITC buffer (20 mM Tris-HCl pH 8.0, 200 mM NaCl, 5% glycerol, 1 mM EDTA and 1 mM TCEP). CUBAN domain at a concentration of 1 mM was injected in volumes of 4 μL into 2 mL of solution containing 50 μM of Nedd8wt, Nedd8 A72R or Ub alone. Two concentrations of NEDD8 (50 and 110 μM) were assayed in independent experiments. Experimental heats were corrected by subtracting the blank measurements and analysed using the ORIGIN software package (MicroCal LCC). Binding constants and other thermodynamic parameters were calculated by fitting the integrated titration data assuming a single binding site.

Circular dichroism

The CD measurements were performed on a Jasco CD spectrophotometer (Jasco Europe S.R.L., Cremella, Italy) using a 0.1 cm path length cell cuvette. The CUBAN domain concentration was of about 50 μM in H_2O. The CD spectra were scanned in the far UV spectral region from 200 to 260 nm, using a step resolution of 0.2 nm and a speed scan for spectra collection of 20 $nm \cdot min^{-1}$. The spectra obtained are the average of four scans at room temperature. An estimate of secondary structure elements content was obtained from K2D3, a web server for CD data prediction [45].

NMR assignments and structure determination of the CUBAN domain

^{15}N-labelled and -unlabelled CUBAN domain was suspended separately in 90 : 10 H_2O/D_2O mixture at 1.3 mM. The uniformly ^{15}N-labelled sample was used in order to acquire 3D and 2D heteronuclear NMR experiments. The unlabelled sample was used for 2D homonuclear NMR experiments. All NMR experiments used for structure determination were performed on a Bruker Avance (Bruker Italy, Milano, Italy) operating at 700.13 MHz. NMR, data were processed with Bruker software TOPSPIN 3.1 (NMR data handling of Bruker Italy) and analysed with NMR*View*. Sequence-specific assignments of backbone and side-chain ^{1}H and ^{15}N resonances were performed using the standard ^{15}N-edited 3D TOCSY-HSQC (τ_{mixing} 40, 90 and 130 ms with 2048 × 64 × 128 complex points) [46–50] ^{15}N

3D NOESY-HSQC (τ_{mixing} 100 and 160 ms with 2048 × 64 × 128 complex points) [49] and 2D homunclear NOESY (τ_{mixing} 250 ms with 4096 × 360 complex points) experiments [51]. Intra- and intermolecular NOE distance constraints were derived from 3D heteronuclear ^{15}N-edited NOESY-HSQC and from 2D homonuclear NOESY experiments. Additional restraints were used such as torsion angles of backbone, φ and ψ, and hydrogen bond, defined as $r_{HNi-Oi+4}$ = 1.7 ... 2.0 Å and $r_{Ni-Oi+4}$ = 2.7 ... 3.0 Å. The CNS software was used for structure calculation [52]. From 100 structures generated as output in the simulated annealing, a cluster of 12 structures with an average distance violation RMSD of 0.5 Å was selected. The CUBAN domain structure energy minimization was performed with GROMACS package. Evaluation of the domain structure quality was performed with PROCHECK-NMR and WHAT-IF programs.

Chemical shift perturbations measurement

The CSP analysis [34] was carried out following the changes in the ^{15}N HSQC spectra of ^{15}N-labelled KHNYN in the presence of NEDD8 and of ^{15}N-labelled NEDD8 upon increasing unlabelled CUBAN separately. The labelled and unlabelled protein concentrations, at a molar ratio of 1 : 1, were typically about 200 μM. Two-dimensional ^{15}N-HSQC was acquired at 298K with a Bruker Avance operating at 700.13 MHz. All spectra were processed and analysed with Bruker software TOPSPIN 3.1. The proton and nitrogen CSPs of the labelled species are defined as the difference between the chemical shift of the protein in the bound and the free states (see Eqns 1, 2) [34].

$$CSP_H = \delta^1H_{bound} - \delta^1H_{free} \quad (1)$$

$$CSP_N = \delta^{15}N_{bound} - \delta^{15}N_{free} \quad (2)$$

The combined perturbation $CSP_{(H+N)}$ is given:

$$CSP_{H+N} = \sqrt{\frac{1}{2}[CSP_H^2 + (0.14 \cdot CSP_N^2)]}$$

Molecular dynamics

The energy of both CUBAN domain and CUBAN–NEDD8 complex structures was minimized in water using the GROMACS package. The molecular dynamics simulation was performed with GROMACS 4.5 [53] using the AMBER03 protein, nucleic AMBER94 [54] force field and the TIP3P model for water molecules. The simulations were performed on a total time of 1 ns for KHNYN and 0.6 ns for the CUBAN–NEDD8 complex structure. The cut-off radius was set at 0.8 nm for electrostatic interactions and 0.8 nm for Lennard-Jones interactions. Long-range electrostatic interactions were treated using the particle-mesh Ewald (PME) method [54]. Temperature coupling was performed with a Nose–Hoover thermostat [55] and pressure coupling was carried out with the Parrinello–Rahman barostat [56]. The calculations were performed on a Linux PC presenting an AMD Athlon(tm) II X2 260 Processor × 2 at a rate of about 19.6 ns day^{-1}.

Molecular docking

The HADDOCK server was used to determinate the structure of CUBAN-NEDD8 complex. CSP data obtained from NMR titrations experiments of ^{15}N-labelled KHNYN and ^{15}N-labelled NEDD8 were used to drive the docking process. This information is introduced as an ambiguous distance between all residues involved in the interaction [54]. The CUBAN–NEDD8 complex structure energy was minimized with GROMACS software.

Acknowledgements

We thank COST Action PROTEOSTASIS BM1307 members for supporting this work and Vladimir Rogov, Enchev Radoslav Ivanof, Pier Paolo di Fiore and Elena Maspero for technical support and useful discussion. This work was supported by the European Research Council grant No. 322749 DEPTH to GC and by the grant from Italian Association for Cancer Research (AIRC) to GC and the AIRC grant to SP (IG15637). MP acknowledges support from Department of Chemical Sciences and Technologies of Tor Vergata University for supporting maintenance of instrumentation by external financial supports.

Conflict of interest

The authors declare that they have no conflicts of interest with the contents of this article.

Author contributions

Conceptualization, ES, GC and LC; design, methodology and project supervision, ES; data acquisition and analysis, ES, WM, RN, EV, AM, MI and RP; interpretation of data, ES, MP, GC and SP; writing the paper, ES and MP; critical revision of the manuscript, SP, GC and LC. All authors approved the final version of the manuscript.

References

1 Ravid T & Hochstrasser M (2008) Diversity of degradation signals in the ubiquitin-proteasome system. *Nat Rev Mol Cell Biol* **9**, 679–690.

2 Mayer RJ, Landon M & Layfield R (1998) Ubiquitin superfolds: intrinsic and attachable regulators of cellular activities? *Fold Des* **3**, R97–R99.
3 Schwechheimer C (2018) NEDD8 — its role in the regulation of Cullin-RING ligases. *Curr Opin Plant Biol* **45**, 112–119.
4 Huang DT, Miller DW, Mathew R, Cassell R, Holton JM, Roussel MF & Schulman BA (2004) A unique E1-E2 interaction required for optimal conjugation of the ubiquitin-like protein NEDD8. *Nat Struct Mol Biol* **11**, 927–935.
5 Huang DT, Paydar A, Zhuang M, Waddell MB, Holton JM & Schulman BA (2005) Structural basis for recruitment of Ubc12 by an E2 binding domain in NEDD8's E1. *Mol Cell* **17**, 341–350.
6 Huang DT, Hunt HW, Zhuang M, Ohi MD, Holton JM & Schulman BA (2007) Basis for a ubiquitin-like protein thioester switch toggling E1-E2 affinity. *Nature* **445**, 394–398.
7 Huang DT, Zhuang M, Ayrault O & Schulman BA (2008) Identification of conjugation specificity determinants unmasks vestigial preference for ubiquitin within the NEDD8 E2. *Nat Struct Mol Biol* **15**, 280–287.
8 Souphron J, Waddell MB, Paydar A, Tokgöz-Gromley Z, Roussel MF & Schulman BA (2008) Structural dissection of a gating mechanism preventing misactivation of ubiquitin by NEDD8's E1. *Biochemistry* **47**, 8961–8969.
9 Walden H, Podgorski MS, Huang DT, Miller DW, Howard RJ, Minor DL, Holton JM & Schulman BA (2003) The structure of the APPBP1-UBA3-NEDD8-ATP complex reveals the basis for selective ubiquitin-like protein activation by an E1. *Mol Cell* **12**, 1427–1437.
10 Whitby FG, Xia G, Pickart CM & Hill CP (1998) Crystal structure of the human ubiquitin-like protein NEDD8 and interactions with ubiquitin pathway enzymes. *J Biol Chem* **273**, 34983–34991.
11 Shen L-N, Liu H, Dong C, Naismith JH & Hay RT (2005) Structural basis of NEDD8 ubiquitin discrimination by the deNEDDylating enzyme NEDP1. *EMBO J* **24**, 1341–1351.
12 Rabut G & Peter M (2008) Function and regulation of protein neddylation. "Protein modifications: beyond the usual suspects" review series. *EMBO Rep* **9**, 969–976.
13 Singh RK, Zerath S, Kleifeld O, Scheffner M, Glickman MH & Fushman D (2012) Recognition and cleavage of related to ubiquitin 1 (Rub1) and Rub1-ubiquitin chains by components of the ubiquitin-proteasome system. *Mol Cell Proteomics* **11**, 1595–1611.
14 Oved S, Mosesson Y, Zwang Y, Santonico SK, Marmor MD, Kochupurakkal BS, Katz M, Lavi S, Cesareni G & Yarden Y (2006) Conjugation to Nedd8 instigates ubiquitylation and down-regulation of activated receptor tyrosine kinases. *J Biol Chem* **281**, 21640–21651.
15 Besten WD, Verma R, Kleiger G, Oania RS & Deshaies RJ (2012) NEDD8 links cullin-RING ubiquitin ligase function to the p97 pathway. *Nat Struct Mol Biol* **19**, 511–516.
16 Bandau S, Knebel A, Gage ZO, Wood NT & Alexandru G (2012) UBXN7 docks on neddylated cullin complexes using its UIM motif and causes HIF1α accumulation. *BMC Biol* **10**, 36.
17 Kelsall IR, Duda DM, Olszewski JL, Hofmann K, Knebel A, Langevin F, Wood N, Wightman M, Schulman BA & Alpi AF (2013) TRIAD1 and HHARI bind to and are activated by distinct neddylated Cullin-RING ligase complexes. *EMBO J* **32**, 2848–2860.
18 Ma T, Chen Y, Zhang F, Yang C-Y, Wang S & Yu X (2013) RNF111-dependent neddylation activates DNA damage-induced ubiquitination. *Mol Cell* **49**, 897–907.
19 Tanaka T, Kawashima H, Yeh ETH & Kamitani T (2003) Regulation of the NEDD8 conjugation system by a splicing variant, NUB1L. *J Biol Chem* **278**, 32905–32913.
20 Schmidtke G, Kalveram B, Weber E, Bochtler P, Lukasiak S, Hipp MS & Groettrup M (2006) The UBA domains of NUB1L are required for binding but not for accelerated degradation of the ubiquitin-like modifier FAT10. *J Biol Chem* **281**, 20045–20054.
21 Xie P, Zhang M, He S, Lu K, Chen Y, Xing G, Lu Y, Liu P, Li Y, Wang S *et al.* (2014) The covalent modifier Nedd8 is critical for the activation of Smurf1 ubiquitin ligase in tumorigenesis. *Nat Commun* **5**, 3733.
22 He S, Cao Y, Xie P, Dong G & Zhang L (2017) The Nedd8 non-covalent binding region in the Smurf HECT domain is critical to its ubiquitn ligase function. *Sci Rep* **7**, 41364.
23 Zucconi A, Panni S, Paoluzi S, Castagnoli L, Dente L & Cesareni G (2000) Domain repertoires as a tool to derive protein recognition rules. *FEBS Lett* **480**, 49–54.
24 Fenner BJ, Scannell M & Prehn JHM (2009) Identification of polyubiquitin binding proteins involved in NF-κB signaling using protein arrays. *Biochim Biophys Acta* **1794**, 1010–1016.
25 Sharma P, Murillas R, Zhang H & Kuehn MR (2010) N4BP1 is a newly identified nucleolar protein that undergoes SUMO-regulated polyubiquitylation and proteasomal turnover at promyelocytic leukemia nuclear bodies. *J Cell Sci* **123**, 1227–1234.
26 Hjerpe R, Thomas Y, Chen J, Zemla A, Curran S, Shpiro N, Dick LR & Kurz T (2012) Changes in the ratio of free NEDD8 to ubiquitin triggers NEDDylation by ubiquitin enzymes. *Biochem J* **441**, 927–936.

27 Anantharaman V & Aravind L (2006) The NYN domains: novel predicted RNAses with a PIN domain-like fold. *RNA Biol* **3**, 18–27.
28 Cuff JA & Barton GJ (2000) Application of multiple sequence alignment profiles to improve protein secondary structure prediction. *Proteins* **40**, 502–511.
29 Schultz J, Milpetz F, Bork P & Ponting CP (1998) SMART, a simple modular architecture research tool: identification of signaling domains. *Proc Natl Acad Sci USA* **95**, 5857–5864.
30 Letunic I, Doerks T & Bork P (2015) SMART: recent updates, new developments and status in 2015. *Nucleic Acids Res* **43**, D257–D260.
31 Wimuttisuk W & Singer JD (2007) The Cullin3 ubiquitin ligase functions as a Nedd8-bound heterodimer. *Mol Biol Cell* **18**, 899–909.
32 Chew E-H, Poobalasingam T, Hawkey CJ & Hagen T (2007) Characterization of cullin-based E3 ubiquitin ligases in intact mammalian cells–evidence for cullin dimerization. *Cell Signal* **19**, 1071–1080.
33 Tang X, Orlicky S, Lin Z, Willems A, Neculai D, Ceccarelli D, Mercurio F, Shilton BH, Sicheri F & Tyers M (2007) Suprafacial orientation of the SCFCdc4 dimer accommodates multiple geometries for substrate ubiquitination. *Cell* **129**, 1165–1176.
34 Williamson MP (2013) Using chemical shift perturbation to characterise ligand binding. *Prog Nucl Magn Reson Spectrosc* **73**, 1–16.
35 Sakata E, Yamaguchi Y, Miyauchi Y, Iwai K, Chiba T, Saeki Y, Matsuda N, Tanaka K & Kato K (2007) Direct interactions between NEDD8 and ubiquitin E2 conjugating enzymes upregulate cullin-based E3 ligase activity. *Nat Struct Mol Biol* **14**, 167–168.
36 Kulathu Y & Komander D (2012) Atypical ubiquitylation – the unexplored world of polyubiquitin beyond Lys48 and Lys63 linkages. *Nat Rev Mol Cell Biol* **13**, 508–523.
37 Hurley JH, Lee S & Prag G (2006) Ubiquitin-binding domains. *Biochem J* **399**, 361–372.
38 Scott DC, Sviderskiy VO, Monda JK, Lydeard JR, Cho SE, Harper JW & Schulman BA (2014) Structure of a RING E3 trapped in action reveals ligation mechanism for the ubiquitin-like protein NEDD8. *Cell* **157**, 1671–1684.
39 Ikeda F & Dikic I (2008) Atypical ubiquitin chains: new molecular signals. 'Protein modifications: beyond the usual suspects' review series.. *EMBO Rep* **9**, 536–542.
40 Baber JL, Libutti D, Levens D & Tjandra N (1999) High precision solution structure of the C-terminal KH domain of heterogeneous nuclear ribonucleoprotein K, a c-myc transcription factor. *J Mol Biol* **289**, 949–962.
41 García-Mayoral MF, Hollingworth D, Masino L, Díaz-Moreno I, Kelly G, Gherzi R, Chou C-F, Chen C-Y & Ramos A (2007) The structure of the C-terminal KH domains of KSRP reveals a noncanonical motif important for mRNA degradation. *Structure* **15**, 485–498.
42 Santi E, Capone S, Mennuni C, Lahm A, Tramontano A, Luzzago A & Nicosia A (2000) Bacteriophage lambda display of complex cDNA libraries: a new approach to functional genomics. *J Mol Biol* **296**, 497–508.
43 Santonico PS, Falconi M, Castagnoli L & Cesareni G (2007) Binding to DPF-motif by the POB1 EH domain is responsible for POB1-Eps15 interaction. *BMC Biochem* **8**, 29.
44 Weber DJ, Gittis AG, Mullen GP, Abeygunawardana C, Lattman EE & Mildvan AS (1992) NMR docking of a substrate into the X-ray structure of staphylococcal nuclease. *Proteins* **13**, 275–287.
45 Louis-Jeune C, Andrade-Navarro MA & Perez-Iratxeta C (2012) Prediction of protein secondary structure from circular dichroism using theoretically derived spectra. *Proteins* **80**, 374–381.
46 Bax A (1985) MLEV-17-based two-dimensional homonuclear magnetization transfer spectroscopy. *J Magn Reson* **65**, 355–360.
47 Davis A (2004) Experiments for recording pure-absorption heteronuclear correlation spectra using pulsed field gradients. *J Magn Reson* **98**, 207–216.
48 Palmer A (1992) Sensitivity improvement in proton-detected two-dimensional heteronuclear correlation NMR spectroscopy. *J Magn Reson* **93**, 151–170.
49 Kay L (1992) Pure absorption gradient enhanced heteronuclear single quantum correlation spectroscopy with improved sensitivity. *J Am Chem Soc* **114**, 10663–10665.
50 Schleucher J (2003) Coherence selection by gradients without signal attenuation: application to the three-dimensional HNCO experiment. *Angew Chem* **32**, 1489–1491.
51 Piotto M & Sklenar V (1992) Gradient-tailored excitation for single-quantum NMR spectroscopy of aqueous solutions. *J Biomol NMR* **2**, 661–666.
52 Brünger AT, Adams PD, Clore GM, DeLano WL, Gros P, Grosse-Kunstleve RW, Jiang JS, Kuszewski J, Nilges M, Pannu NS *et al.* (1998) Crystallography & NMR system: a new software suite for macromolecular structure determination. *Acta Crystallogr D Biol Crystallogr* **54**, 905–921.
53 Hess B, Kutzner C, van der Spoel D & Lindahl E (2008) GROMACS 4: algorithms for highly efficient, load-balanced, and scalable molecular simulation. *J Chem Theory Comput* **4**, 435–447.
54 Duan Y, Wu C, Chowdhury S, Lee MC, Xiong G, Zhang W, Yang R, Cieplak P, Luo R, Lee T *et al.* (2003) A point-charge force field for molecular mechanics simulations of proteins based on condensed-phase quantum mechanical calculations. *J Comput Chem* **24**, 1999–2012.

55 Essmann U, Perera L, Berkowitz ML, Darden T, Lee H & Pedersen LG (1995) A smooth particle mesh Ewald method. *J Chem Phys* **103**, 8577–8593.
56 Cheng A (1996) Application of the Nosé-Hoover chain algorithm to the study of protein dynamics *J Phys Chem* **100**, 1927–1937.
57 Sievers F, Wilm A, Dineen DG, Gibson TJ, Karplus K, Li W, Lopez R, McWilliam H, Remmert M, Söding J *et al.* (2011) Fast, scalable generation of high-quality protein multiple sequence alignments using Clustal Omega. *Mol Syst Biol* **7**, 539. https://doi.org/10.1038/msb.2011.75
58 Sievers F & Higgins DG (2018) Clustal Omega for making accurate alignments of many protein sciences. *Protein Sci* **27**, 135–145.

Supporting information

Additional supporting information may be found online in the Supporting Information section at the end of the article.

Table S1. NMR structural statistics obtained for the family of 10 (out of the 12) CUBAN structures. The detailed description of the assigned atoms and the number of short-, medium- and long-range NOEs are reported.